



HAL
open science

The ASSET intercomparison of ozone analyses: method and first results

A. J. Geer, W. A. Lahoz, Slimane Bekki, N. Bormann, Q. Errera, H. J. Eskes, D. Fonteyn, D. R. Jackson, M. N. Juckes, S. Massart, et al.

► To cite this version:

A. J. Geer, W. A. Lahoz, Slimane Bekki, N. Bormann, Q. Errera, et al.. The ASSET intercomparison of ozone analyses: method and first results. Atmospheric Chemistry and Physics Discussions, 2006, 6 (3), pp.4495-4577. hal-00327911

HAL Id: hal-00327911

<https://hal.science/hal-00327911>

Submitted on 18 Jun 2008

HAL is a multi-disciplinary open access archive for the deposit and dissemination of scientific research documents, whether they are published or not. The documents may come from teaching and research institutions in France or abroad, or from public or private research centers.

L'archive ouverte pluridisciplinaire **HAL**, est destinée au dépôt et à la diffusion de documents scientifiques de niveau recherche, publiés ou non, émanant des établissements d'enseignement et de recherche français ou étrangers, des laboratoires publics ou privés.

**Intercomparison of
ozone analyses**

A. J. Geer et al.

The ASSET intercomparison of ozone analyses: method and first results

**A. J. Geer¹, W. A. Lahoz¹, S. Bekki², N. Bormann³, Q. Errera⁴, H. J. Eskes⁵,
D. Fonteyn⁴, D. R. Jackson⁶, M. N. Juckes⁷, S. Massart⁸, V.-H. Peuch⁹,
S. Rharmili², and A. Segers⁵**

¹Data Assimilation Research Centre, University of Reading, Reading, UK

²CNRS Service Aeronomie, Université Pierre et Marie Curie, Paris, France

³European Centre for Medium-Range Weather Forecasts, Reading, UK

⁴Institut d'Aéronomie Spatiale de Belgique, Brussels, Belgium

⁵Royal Netherlands Meteorological Institute, De Bilt, The Netherlands

⁶Met Office, Exeter, UK

⁷British Atmospheric Data Centre, Rutherford Appleton Laboratory, Chilton, nr Didcot, UK

⁸CERFACS, Toulouse, France

⁹CNRM-GAME, Météo-France and CNRS URA 1357, Toulouse, France

Received: 6 February 2006 – Accepted: 7 March 2006 – Published: 7 June 2006

Correspondence to: A. J. Geer (alan.geer@ecmwf.int)

Title Page

Abstract

Introduction

Conclusions

References

Tables

Figures

◀

▶

◀

▶

Back

Close

Full Screen / Esc

Printer-friendly Version

Interactive Discussion

EGU

Abstract

This paper examines 11 sets of ozone analyses from 7 different data assimilation systems. Two are numerical weather prediction (NWP) systems based on general circulation models (GCMs); the other five use chemistry transport models (CTMs). These systems contain either linearised or detailed ozone chemistry, or no chemistry at all. In most analyses, MIPAS (Michelson Interferometer for Passive Atmospheric Sounding) ozone data are assimilated. Two examples assimilate SCIAMACHY (Scanning Imaging Absorption Spectrometer for Atmospheric Chartography) observations. The analyses are compared to independent ozone observations covering the troposphere, stratosphere and lower mesosphere during the period July to November 2003.

Through most of the stratosphere (50 hPa to 1 hPa), biases are usually within $\pm 10\%$ and standard deviations less than 10% compared to ozonesondes and HALOE (Halogen Occultation Experiment). Biases and standard deviations are larger in the upper-troposphere/lower-stratosphere, in the troposphere, the mesosphere, and the Antarctic ozone hole region. In these regions, some analyses do substantially better than others, and this is mostly due to differences in the models. At the tropical tropopause, many analyses show positive biases and excessive structure in the ozone fields, likely due to known deficiencies in assimilated tropical wind fields and a degradation in MIPAS data at these levels. In the southern hemisphere ozone hole, only the analyses which correctly model heterogeneous ozone depletion are able to reproduce the near-complete ozone destruction over the pole. In the upper-stratosphere and mesosphere (above 5 hPa), some ozone photochemistry schemes caused large but easily remedied biases. The diurnal cycle of ozone in the mesosphere is not captured, except by the one system that includes a detailed treatment of mesospheric chemistry.

In general, similarly good results are obtained no matter what the assimilation method (Kalman filter, three or four dimensional variational methods, direct inversion), or system (CTM or NWP system) and this in part reflects the generally good quality of the MIPAS ozone observations. Analyses based on SCIAMACHY total column are

Intercomparison of ozone analyses

A. J. Geer et al.

Title Page

Abstract

Introduction

Conclusions

References

Tables

Figures

◀

▶

◀

▶

Back

Close

Full Screen / Esc

Printer-friendly Version

Interactive Discussion

almost as good as the MIPAS analyses; analyses based on SCIAMACHY limb profiles are worse in some areas, due to problems in the SCIAMACHY retrievals.

Using the analyses as a transfer standard, and treating MIPAS observations as point retrievals, it is seen that MIPAS is $\sim 5\%$ higher than HALOE in the mid and upper stratosphere and mesosphere (above 30 hPa), and of order 10% higher than ozonesonde and HALOE in the lower stratosphere (100 hPa to 30 hPa).

1 Introduction

The Assimilation of ENVISAT Data (ASSET, <http://darc.nerc.ac.uk/asset>) project aims to provide analyses of atmospheric chemical constituents, based on the assimilation of observations from the ENVISAT satellite, and to develop chemical weather and UV forecasting capabilities. Data are assimilated into a variety of different systems, including chemical transport models (CTMs) with detailed chemistry or simple chemistry, and Numerical Weather Prediction (NWP) systems based on General Circulation Models (GCMs), either with simple chemistry, or coupled to detailed-chemistry CTMs. Data assimilation techniques (see e.g., [Kalnay, 2003](#)) include three and four-dimensional variational data assimilation (3D-Var and 4D-Var) and the Kalman Filter (KF). It is hoped that, by confronting these various models and techniques with the newly available ENVISAT observations, it will be possible both to gain an understanding of their strengths and weaknesses, and to make new developments. A number of ozone analyses have been created within the ASSET project; this paper compares them to independent observations and to ozone analyses from outside the project. There have been a number of previous intercomparisons between the ozone distributions in different CTMs (e.g., [Bregman et al., 2001](#); [Roelofs et al., 2003](#)) but this is the first time ozone analyses have been compared.

Datasets of assimilated ozone will be useful for research and monitoring of ozone depletion (e.g., [WMO, 2003](#)), tropospheric pollution, and UV fluxes, and beyond this, ozone assimilation is expected to bring a number of benefits in NWP. First, in the upper-

Intercomparison of ozone analyses

A. J. Geer et al.

Title Page

Abstract

Introduction

Conclusions

References

Tables

Figures

◀

▶

◀

▶

Back

Close

Full Screen / Esc

Printer-friendly Version

Interactive Discussion

**Intercomparison of
ozone analyses**A. J. Geer et al.

[Title Page](#)[Abstract](#)[Introduction](#)[Conclusions](#)[References](#)[Tables](#)[Figures](#)[◀](#)[▶](#)[◀](#)[▶](#)[Back](#)[Close](#)[Full Screen / Esc](#)[Printer-friendly Version](#)[Interactive Discussion](#)

5 troposphere/lower-stratosphere (UTLS), ozone has a photochemical relaxation time of order 100 days, and it can be used as a tracer to infer atmospheric motions using 4D-Var (e.g., Riishøjgaard, 1996; Peuch et al., 2000). Second, NWP systems have typically used a zonal mean ozone climatology in modelling heating rates and in the forward radiative transfer calculations used in the assimilation of satellite radiances such as those from the Atmospheric Infrared Sounder (AIRS). An estimate of the true 3-D ozone distribution is likely to improve these calculations. Experiments at ECMWF found that variations in ozone amounts of ~10 to 20% could result in changes in modelled tropical UTLS temperatures of up to 4 K (Cariolle and Morcrette, 2006). The diurnal cycle of ozone is important in the middle atmosphere. Model runs with diurnally varying ozone show temperature differences of up to 3 K in the stratosphere, compared to those with climatological ozone (Sassi et al., 2005). A prognostic ozone field also allows the modelling of feedbacks between radiation, chemistry and dynamics, and this is expected to improve forecasts, especially over longer timescales. However, no study has yet found a clear benefit in terms of forecast scores (e.g., Morcrette, 2003). Finally, in order to simulate a good ozone distribution, models used in assimilation systems must be able to simulate stratospheric transport well; problems are often revealed when these models are confronted with real observations (e.g., Geer et al., 2006).

20 Different approaches can be used for ozone data assimilation and the choice will vary depending on the application. Chemical transport models typically use operationally-produced analyses of wind and temperature (such as those from ECMWF) to advect chemical constituents. If chemistry is treated approximately, these models are extremely fast and can be used to assimilate many months of observations in a few days on a desktop computer. Including a detailed chemistry scheme, with dozens of constituents and hundreds of reactions, allows a more accurate simulation of the ozone distribution, but is slower. The CTM approach has been very popular for ozone analysis systems (e.g., Fisher and Lary, 1995; Khattatov et al., 2000; Elbern and Schmidt, 2001; Errera and Fonteyn, 2001; Štajner et al., 2001; Chipperfield et al., 2002; Fierli et al., 2002; Cathala et al., 2003; Eskes et al., 2003, 2005a; El Amraoui et al., 2004;

Massart et al., 2005; Segers et al., 2005a; Wargan et al., 2005). It is also possible to introduce a prognostic ozone field directly into an NWP system (e.g., Struthers et al., 2002; Dethof and Hólm, 2004; Geer et al., 2006), but ozone assimilation then becomes part of a very large operational system, requiring a supercomputer. Much work is still
5 required to confirm the proposed benefits of including ozone directly into NWP systems. One alternative approach is to couple CTMs, with a detailed description of chemistry, to GCM-based NWP systems, such that feedbacks between chemistry, dynamics and radiation can be maintained.

Current operational satellite ozone observations include the Total Ozone Mapping Spectrometer (TOMS), measuring total column ozone, and the Solar Backscatter Ultraviolet (SBUV) instrument (e.g., Bhartia et al., 1996), which produces vertical profiles. ENVISAT, launched in 2002, provides the instruments MIPAS (Michelson Interferometer for Passive Atmospheric Sounding), SCIAMACHY (Scanning Imaging Absorption Spectrometer for Atmospheric Chartography) and GOMOS (Global Ozone Monitoring by Occultation of Stars). Between them, these instruments measure many species beyond ozone, and vertical resolution is much improved over the operational instruments. For example, MIPAS has roughly twice the vertical resolution of SBUV in the stratosphere (see e.g. Fig. 2, Wargan et al., 2005). The ASSET project is based around
10 assimilating the data from ENVISAT. The EOS-Aura satellite, launched in 2004, has instruments with similar capabilities. Research instruments such as those on ENVISAT and Aura do, however, have a limited lifetime and data products are not always available quickly enough to be included in operational NWP schedules. Hence research satellite data is often best used for re-analyses, and to help improve models and assimilation systems such that the operational observations, such as SBUV, may be assimilated
15 more successfully.

For this intercomparison, ozone analyses have been made for the period July to November 2003, chosen because of the availability of good quality MIPAS data. This period included one of the largest ozone holes on record (e.g., Dethof, 2003a), caused by relatively low temperatures in a fairly stable southern hemisphere (SH) polar vortex,

**Intercomparison of
ozone analyses**A. J. Geer et al.

Title Page

Abstract

Introduction

Conclusions

References

Tables

Figures

◀

▶

◀

▶

Back

Close

Full Screen / Esc

Printer-friendly Version

Interactive Discussion

which was destroyed by the usual top-down break-up during October and November (Lahoz et al., 2006).

Eleven analysis runs are included in the intercomparison, made using seven different systems, summarised in Table 1. Two climatology-derived products are also included in the intercomparison. All but two analysis runs assimilate MIPAS ozone data; the others assimilate SCIAMACHY. Both CTMs and GCMs are represented, and ozone chemistry may or may not be modelled. If included, it is done either by highly detailed reaction schemes or via a parametrization often known as a Cariolle scheme (e.g., Cariolle and Déqué, 1986; McLinden et al., 2000; McCormack et al., 2004). The Cariolle scheme is a linearisation of ozone photochemistry around an equilibrium state, using parameters derived from a more detailed model.

Most of the analysis systems are focused on the stratosphere, but the scope of the comparison spans from the troposphere to the mesosphere. Analyses are interpolated from their native resolution onto a common grid and then compared to independent ozone data from Halogen Occultation Experiment (HALOE), ozonesondes and TOMS, and to MIPAS. Most data, figures, and code are being made publicly available via the project website (<http://darc.nerc.ac.uk/asset>).

This paper introduces the intercomparison project, the method used, the independent data sources, and the analysis systems involved. It outlines many of the initial results, such as problems found with some implementations of linearised ozone chemistry schemes, and it draws initial conclusions on the various different methods used. There is not scope in this paper for detailed comparisons, such as between different types of chemistry schemes, or between 3D-Var and 4D-Var. These are anyway best performed in an experimental setting within a single assimilation system. However, the intercomparison provides a framework under which these results, and their significance, can be assessed by comparison to a variety of other assimilation approaches and systems. These more detailed results will be described in further papers.

Intercomparison of ozone analyses

A. J. Geer et al.

Title Page

Abstract

Introduction

Conclusions

References

Tables

Figures

◀

▶

◀

▶

Back

Close

Full Screen / Esc

Printer-friendly Version

Interactive Discussion

2 Analyses

Before describing in detail the analyses and climatologies in the intercomparison, we show examples of the ozone fields at 68 hPa on 31 August 2003 (Fig. 1). Sunlight has started to return to high latitudes after the winter, triggering the depletion of ozone in a ring around the pole (see e.g., WMO, 2003). Sunlight has not yet returned to the pole itself. The ring of higher ozone (3 to 5 ppm) at about 45° S is the remainder of ozone that has descended throughout the SH high latitudes during the winter, from levels higher in the atmosphere where ozone amounts are greater. It is clear that at 68 hPa all the analyses show broadly similar and (from Sect. 5) realistic structures. Compared to the others, the KNMI SCIAMACHY profile analyses have a bias; due to a lack of observations before October they are based principally on the free-running model.

2.1 ECMWF

Ozone observations have been assimilated into the operational ECMWF analyses (<http://www.ecmwf.int>) since April 2002. During 2003, GOME columns and SBUV profiles were assimilated, though in August and September 2003, there was very limited availability of GOME data. MIPAS was assimilated operationally from from 7 October 2003 until 25 March 2004. Here we consider two datasets: (a) the operational analyses and (b) a dataset that includes assimilated MIPAS ozone throughout the July–November period, based on a pre-operational test suite before 7th October, and operational data after 7 October (Dethof, 2003a). In all cases, the MIPAS data is version 4.59 of the Near Real Time product. Gross outliers in the MIPAS retrievals are rejected based on a comparison against the background ozone. Variational quality control is also applied (Andersson and Järvinen, 1999).

The GCM in use when the analyses were made had a horizontal resolution of T511 (~50 km) and 60 levels in the vertical, from the surface up to 0.1 hPa. Ozone was advected using a semi-Lagrangian transport scheme. Ozone chemistry was parametrized with version 1.2 of the Cariolle scheme (Cariolle and Déqué, 1986; Dethof and Hólm,

Intercomparison of ozone analyses

A. J. Geer et al.

Title Page

Abstract

Introduction

Conclusions

References

Tables

Figures

◀

▶

◀

▶

Back

Close

Full Screen / Esc

Printer-friendly Version

Interactive Discussion

2004), which includes a description of heterogeneous ozone depletion. Climatological ozone (Fortuin and Langematz, 1995), not prognostic ozone, was used for modelling heating rates.

Data assimilation uses 4D-Var (e.g., Rabier et al., 2000). Ozone is assimilated univariately, but it can still affect the dynamical analyses through the 4D-Var method (e.g., Riishøjgaard, 1996) and through the influence of ozone on the assimilation of temperature radiances. Background error correlations are calculated using an ensemble of analyses (Fisher, 2003); background error variances are flow dependent.

2.2 DARC/Met Office

The Met Office NWP system has recently been extended to allow the assimilation of ozone (Jackson and Saunders, 2002; Jackson, 2004) but ozone is not assimilated operationally. Here, MIPAS v4.61 ozone and temperature are assimilated in re-analysis mode, alongside all operational dynamical observations, using a stratosphere/troposphere version of the operational NWP system. The system is that described in Geer et al. (2006), but with a number of improvements to the GCM and no assimilation of HIRS (High resolution infrared radiation sounder) channel 9 ozone radiances.

The assimilating GCM has a horizontal resolution of 3.75° longitude by 2.5° latitude and 50 levels in the vertical, from the surface to ~0.1 hPa. It uses a new dynamical core (Davies et al., 2005) which includes a semi-Lagrangian transport scheme. This gives a better description of the Brewer-Dobson circulation than that seen in Geer et al. (2006). Ozone photochemistry is parametrized by v1.0 of the Cariolle and Déqué (1986) scheme. Improving on Geer et al. (2006), heterogeneous ozone chemistry is now parametrized, using a cold tracer scheme (Eskes et al., 2003). Climatological ozone (Li and Shine, 1995), not the prognostic field, is used for modelling heating rates.

Data assimilation uses 3D-Var (Lorenc et al., 2000). As for ECMWF, ozone is assimilated univariately, but 3D-Var does not infer dynamical information, so the only effect

Intercomparison of ozone analyses

A. J. Geer et al.

Title Page

Abstract

Introduction

Conclusions

References

Tables

Figures

◀

▶

◀

▶

Back

Close

Full Screen / Esc

Printer-friendly Version

Interactive Discussion

of ozone on the dynamical analysis is through its influence on temperature radiance assimilation. Background error covariances are uniform for all latitudes and longitudes, and they are based on the ECMWF vertical covariances. As illustrated in [Geer et al. \(2006\)](#), the MIPAS ozone observations are subject to quality control, but with a lax threshold, so very few observations are rejected.

2.3 KNMI

The Royal Netherlands Meteorological Institute (KNMI) operate a CTM which has been used to assimilate SCIAMACHY ozone data. The CTM uses a subset of 44 of the ECMWF model levels, from the surface to 0.1 hPa, on a 3° longitude by 2° latitude grid. Data assimilation is done using a sub-optimal Kalman Filter (see e.g., [Kalnay, 2003](#)), where the background error variances, but not the correlations, are advected as a tracer. Two different configurations are presented.

The first configuration assimilates total column ozone from SCIAMACHY, retrieved at KNMI using the TOSOMI algorithm (Total Ozone retrieval scheme for SCIAMACHY based on the OMI DOAS algorithm, [Eskes et al., 2005b](#)). The CTM is driven by ECMWF operational analyses of winds and temperatures. Ozone photochemistry is parametrized using the LINOZ scheme ([McLinden et al., 2000](#)), a variant on [Cariolle and Déqué \(1986\)](#). Heterogeneous chemistry uses a cold tracer scheme. For assimilating total column observations, the vertical error correlations are set proportional to the vertical ozone profile. The system is very similar to that described in [Eskes et al. \(2003\)](#).

The second configuration assimilates ozone profiles (IFE v1.6) from the limb-sounding mode of SCIAMACHY into the TM5 model. SCIAMACHY limb profiles are mainly available for October and November 2003; July to September is a free model run apart from a few assimilated profiles in August. The main uncertainty in the SCIAMACHY product is pointing, which has a vertical offset of 1–2 km ([Segers et al., 2005b](#)). All profiles have been shifted in the vertical to get the best match with model forecasts prior to analysis. Ozone chemistry is parameterized using [Cariolle and Déqué \(1986\)](#)

Intercomparison of ozone analyses

A. J. Geer et al.

Title Page

Abstract

Introduction

Conclusions

References

Tables

Figures

◀

▶

◀

▶

Back

Close

Full Screen / Esc

Printer-friendly Version

Interactive Discussion

v1.0 and a cold-tracer scheme. The CTM is driven by ECMWF short range forecasts at 3 hourly intervals. The system is otherwise similar to that described in Segers et al. (2005a).

2.4 BASCOE

5 The Belgian Assimilation System of Chemical Observations from ENVISAT (BASCOE, <http://www.bascoe.oma.be>) is a 4D-Var assimilation system descended from that described in Errera and Fonteyn (2001). Studies of the Antarctic and Arctic winter using the CTM of BASCOE can be found in Chabrilat et al. (2006)¹ and Daerden et al. (2006)². MIPAS v4.61 ozone (O₃), water vapour (H₂O), nitric acid (HNO₃), nitric
10 dioxide (NO₂), methane (CH₄) and nitrous oxide (N₂O) are assimilated. Observations are subjected to an Optimal Interpolation Quality Check (OIQC, e.g. Gauthier et al., 2003). In practice, the lowest MIPAS ozone observations in the ozone hole are rejected. Observations are also rejected if they fail a check for spurious vertical oscillations in the profile.

15 The model includes 57 chemical species and 4 types of stratospheric PSC particles (ice; supercooled ternary solution, STS; nitric acid trihydrate, NAT; sulphuric acid tetrahydrate, SAT) with a full description of stratospheric chemistry and microphysics of PSCs. All chemical species are advected and interact through 143 gas-phase reactions, 48 photolysis reactions and 9 heterogeneous reactions. To allow for calculating
20 transport of PSCs, size distributions of each type are discretized using 36 bins from 0.002 to 36 μm. PSC microphysics is described by the PSCBox scheme (Larsen et al.,

¹Chabrilat, S. H., Van Roozendaal, M., Daerden, F., Errera, Q., Hendrick, F., Bonjean, S., Wilms-Grabe, W., Wagner, T., Richter, A., and Fonteyn, D.: Quantitative assessment of 3-D PSC-chemistry-transport models by simulation of GOME observations during the Antarctic winter of 2002, in preparation, 2006.

²Daerden, F., Larsen, N., Bonjean S., Chabrilat, S., Errera, Q., and Fonteyn, D.: Synoptic PSCs in recent Polar winters: simulations and comparison to observations, in preparation, 2006.

Intercomparison of ozone analyses

A. J. Geer et al.

Title Page

Abstract

Introduction

Conclusions

References

Tables

Figures

◀

▶

◀

▶

Back

Close

Full Screen / Esc

Printer-friendly Version

Interactive Discussion

2000). In order to improve agreement with MIPAS ozone, O₂ photolysis rates were multiplied by 1.25. This version is referred to as v3d24.

Based on early results of this intercomparison, a new version of BASCOE, v3q33, was produced. Among the changes, v3q33 replaces the full PSC calculation by a parametrization that defines (1) surface area density of ice and NAT when their occurrence is possible and (2) the loss of HNO₃ and H₂O due to sedimentation (Chabrillat et al., 2006¹). Ice PSCs are supposed to exist in the winter/spring polar regions at any grid point where the temperature is colder than 186 K, and NAT PSCs at any grid point where the temperature is colder than 194 K. The surface area density is set to 10⁻⁶ cm²/cm³ in the first case and 10⁻⁷ cm²/cm³ in the second. Additionally in v3q33, O₂ photolysis rates are no longer scaled; this reduces the bias against HALOE but increases it against MIPAS (see Sect. 5.1). Finally, the Arakawa A grid of v3d24 was replaced by a C grid (see e.g., Kalnay, 2003) in v3q33.

The CTM is driven by ECMWF operational analyses of winds and temperatures, and uses a subset of 37 of the ECMWF model levels, from the surface to 0.1 hPa, on a 5° longitude by 3.75° latitude grid.

Data assimilation is done using 4D-Var. The background error standard deviation is set as 20% of the background ozone amount. Though there are no off-diagonal elements in the background error covariances (i.e. no vertical or horizontal correlations), information from MIPAS observations is still spread through the observation operator, as in other systems. Here, it averages the 8 grid points surrounding the measurement point, and the relatively broad horizontal resolution of the grid also helps to spread the information.

2.5 Météo-France/CERFACS

The Météo-France/CERFACS assimilation system is based upon the 3-D CTM MOCAGE and the PALM software (Massart et al., 2005). MIPAS v4.61 ozone data are assimilated, but not beyond 80° of latitude.

The PALM framework is particularly versatile, as both the CTM degree of sophisti-

Intercomparison of ozone analyses

A. J. Geer et al.

Title Page

Abstract

Introduction

Conclusions

References

Tables

Figures

◀

▶

◀

▶

Back

Close

Full Screen / Esc

Printer-friendly Version

Interactive Discussion

cation (for instance, the number of chemical tracers involved, the physical or chemical parametrizations, the horizontal and vertical geometries) and the data assimilation technique can be changed easily; this makes the MOCAGE-PALM system a useful platform for sensitivity studies in chemical data assimilation.

MOCAGE is a flexible tropospheric and stratospheric 3-D CTM developed at Météo-France, offering several configurations of varying computational costs. Two separate configurations are examined here. The first uses linear ozone chemistry, with v2.1 of the Cariolle and Déqué (1986) scheme. The second includes a detailed representation of stratospheric and upper tropospheric chemistry, based upon the REPROBUS chemical scheme (Lefèvre et al., 1994), which comprises 55 transients and species and takes into account heterogeneous chemistry on polar stratospheric clouds (Carslaw et al., 1995; Lefèvre et al., 1998). The REPROBUS chemistry version of MOCAGE has already been used for UTLS assimilation studies (Cathala et al., 2003). A more comprehensive version of MOCAGE, with comprehensive tropospheric chemistry, is run daily in operational mode at Météo-France for chemical weather and air quality applications (Dufour et al., 2004, see daily global forecasts at <http://www.prevoir.org/en>)

MOCAGE relies on a semi-Lagrangian advection scheme (Josse et al., 2004). For the experiments presented here, MOCAGE has a 2° by 2° horizontal resolution and 47 hybrid sigma/pressure levels extending from the surface up to 5 hPa. The meteorological forcings are Météo-France ARPEGE operational meteorological analyses of pressure, winds, temperature and humidity (Courtier et al., 1991), available every 6 h.

Any assimilation algorithm can be seen as a sequence of elementary operations or elementary components that can exchange data (Lagarde et al., 2001). Based on this idea, the CERFACS PALM software (<http://www.cerfacs.fr/~palm>) manages the dynamic launching of the coupled components (forecast model, algebra operators, I/O of observational data) and the parallel data exchanges. The MOCAGE-PALM assimilation system is set up here in a 3D-FGAT configuration (3-D First Guess at Assimilation Time, Fisher and Andersson, 2001). As a first approximation, background error standard deviations are prescribed as 20% of the background ozone amount. In order to

Intercomparison of ozone analyses

A. J. Geer et al.

Title Page

Abstract

Introduction

Conclusions

References

Tables

Figures

◀

▶

◀

▶

Back

Close

Full Screen / Esc

Printer-friendly Version

Interactive Discussion

spread assimilation increments spatially, horizontal background error correlations are modelled using a generalized diffusion operator (Weaver and Courtier, 2001), with a length-scale of 4°; no vertical background error correlations are considered.

2.6 MIMOSA

5 MIMOSA (Modèle Isentrope de transport Mésoéchelle de l'Ozone Stratosphérique par Advection) is a CTM driven by ECMWF operational winds and temperatures (Fierli et al., 2002). MIPAS v4.61 ozone data are assimilated. There is no quality control; all observations are included. There are 16 isentropic levels from 335 K to 1650 K, approximately spanning the stratosphere (~200 hPa to ~1 hPa) and a 1° by 1° latitude-longitude grid. Advection is semi-Lagrangian. The model includes neither ozone chem-
10 istry nor cross-isentropic transport.

Data assimilation is done using a sub-optimal Kalman Filter with advected back-
ground error variances, and uses the Physical Space Assimilation System method (PSAS, e.g. Kalnay, 2003). Background error correlations are flow dependent and
15 anisotropic, specified in terms of distance and the potential vorticity (PV) field. The model error covariance (Q) is diagonal, and proportional to the ozone amount, x , e.g. $Q=(qx)^2$ where $q=0.024 \text{ day}^{-1}$ and has been tuned using χ^2 tests.

ECMWF operational temperature and pressure fields are used to interpolate these isentropic analyses onto pressure levels for this study.

20 2.7 Juckes

These are analyses produced by a direct inversion method (Juckes, 2005), which as-
similates many months of MIPAS v4.61 ozone data by making a single iterative solu-
tion. The physical constraint is based on an isentropic transport equation. Rather than
discretising the predictive equations (which would give a CTM), the product of these
25 equations with their adjoint is discretised. The resulting self-adjoint system of equa-
tions is solved with a multigrid relaxation algorithm. This is equivalent to solving the

Intercomparison of ozone analyses

A. J. Geer et al.

Title Page

Abstract

Introduction

Conclusions

References

Tables

Figures

◀

▶

◀

▶

Back

Close

Full Screen / Esc

Printer-friendly Version

Interactive Discussion

Kalman Smoother with fully advected background error covariances.

Ozone transport is driven by ECMWF operational winds and temperatures, on 13 isentropic levels from 380 K to 3000 K. In the horizontal, a binary thinned latitude-longitude spherical grid is used, giving approximately 2° by 2° resolution. The model error covariance (Q) is diagonal, with a constant value of $0.02 \text{ ppmv}^2/\text{day}^2$. The model includes neither ozone chemistry nor cross-isentropic transport. As for MIMOSA, ECMWF pressure and temperature fields are used for interpolation onto pressure levels in this study.

2.8 Climatology

To contrast with the assimilated ozone fields, we include a climatology-derived product in the comparison. As a minimum, we would expect the analyses to do better than climatology. We combine the Logan (1999) tropospheric ozone climatology with the Fortuin and Kelder (1998) stratospheric ozone climatology. In each case, the climatologies are resolved on a monthly basis.

The Logan (1999) climatology uses ozonesonde, surface in-situ data and the TOMS/Stratospheric Aerosol and Gas Experiment (SAGE) tropospheric residual, to produce a partly 3-D and partly 2-D climatology on 13 levels from 1000 hPa to 100 hPa, covering latitudes from 89° S to 89° N. The Fortuin and Kelder (1998) climatology uses ozonesondes, SBUV and TOMS total ozone, from 1980 to 1991, to produce a 2-D (latitude-pressure) climatology with 19 levels from 1000 hPa to 0.3 hPa and covering latitudes from 80° S to 80° N.

An ozone field was created on the intercomparison common grid, daily at 00Z and 12Z, by interpolating the climatologies linearly in time, and treating the climatologies as representative of the 15th of each month. Beyond the northern and southern limits of the climatologies, horizontal extrapolation was done at constant value. Logan (1999) values were taken for levels at 150 hPa and below, and Fortuin and Kelder (1998) above, up to 0.3 hPa. Figure 1 shows that this results in a zonal distribution which, as expected, does not represent the synoptic features in the ozone field.

Intercomparison of ozone analyses

A. J. Geer et al.

Title Page

Abstract

Introduction

Conclusions

References

Tables

Figures

◀

▶

◀

▶

Back

Close

Full Screen / Esc

Printer-friendly Version

Interactive Discussion

**Intercomparison of
ozone analyses**A. J. Geer et al.

Title Page

Abstract

Introduction

Conclusions

References

Tables

Figures

◀

▶

◀

▶

Back

Close

Full Screen / Esc

Printer-friendly Version

Interactive Discussion

An attempt was made to create a PV-mapped ozone climatology in order to capture synoptic variability in the ozone field, but in comparisons against independent data, it proved no better than the largely zonal mean one described above. The climatology derived by [Randel et al. \(1998\)](#), based on Upper Atmosphere Research satellite (UARS) HALOE and Microwave Limb Sounder (MLS) measurements, is made using equivalent latitude coordinates. This was mapped onto the longitudes, latitudes and times of the intercomparison common grid using ECMWF operational PV fields. Figure 1 indicates that this product is able to capture some of the synoptic variations seen in the analyses, but that the fields are affected by noise in the PV-derived equivalent latitudes. This is a well-known limitation of PV-derived equivalent latitude ([Allen and Nakamura, 2003](#)). In addition, in the mid and upper stratosphere where ozone photochemistry is relatively fast, it can quickly remove any relationship between ozone and PV. See, for example, the filamentation event in [Lahoz et al. \(2006\)](#). Hence, we do not consider the PV-mapped ozone product further in the paper, but it forms part of the set of data and figures available from the website, and it is worth noting the limitations of this approach.

2.9 Comparison of ozone background errors

The background error covariance matrix (e.g., [Kalnay, 2003](#)) is important in determining the weight given to observations in data assimilation. In general, at the observation point, more weight is given to the model as the background error standard deviation becomes smaller compared to the observation error standard deviation. However, the spreading of information away from the observation point is determined by the background error correlations, any observation error correlations (not usually considered), and the observation operator. Here, only the DARC and ECMWF systems include vertical correlations in the background errors. The general impact of observations on the system will also depend on how many observations are rejected by quality control.

We examine the background error standard deviation (i.e. the square root of the diagonal of the background error covariance matrix) from a number of the analysis sys-

tems, and compare it to the MIPAS ozone observation error standard deviation (Fig. 2). In each case these have been normalised by the climatological ozone amount (see Sect. 4 for the method). The comparison is done to illustrate the varied approaches to background error modelling, and to give some indication of the weight assigned to observations in the different systems. As already noted, however, many other factors affect the observations' weight in the final analysis.

Figure 2 shows large differences in the ozone background error standard deviations assumed in the assimilation systems. In the mid and upper stratosphere (levels above 30 hPa), DARC and ECMWF background error standard deviations are less than 5% of the ozone field, whereas the BASCOE and (to 5 hPa) Météo-France/CERFACS systems are typically 20%. This suggests the DARC and ECMWF analyses give less weight to observations at these levels. MIPAS observation errors are markedly larger at the tropical tropopause, and all the systems are likely to give relatively lower weight to MIPAS observations here than in the rest of the stratosphere. Work is ongoing to understand the large differences between systems.

3 Ozone observations

3.1 MIPAS

All analyses examined here assimilate MIPAS ozone, except the KNMI analyses, which assimilate SCIAMACHY. Typically, assimilation systems produce observation minus first guess (O-F) statistics that are used for monitoring biases between the observations and the models, and checking that statistical assumptions are valid in the assimilation algorithm (e.g., Talagrand, 2003; Štajner et al., 2004). Here, instead of using the many different formats of O-F produced by individual systems, we simply compare the common-gridded analysis products to MIPAS, similarly to the way we compare to independent HALOE data.

MIPAS is an interferometer for measuring infrared emissions from the atmospheric

Intercomparison of ozone analyses

A. J. Geer et al.

Title Page

Abstract

Introduction

Conclusions

References

Tables

Figures

◀

▶

◀

▶

Back

Close

Full Screen / Esc

Printer-friendly Version

Interactive Discussion

limb (Fischer and Oelhaf, 1996). MIPAS operational data are available between July 2002 and March 2004, after which instrument problems meant it could only be used on an occasional basis. The operational measurements were made along 17 discrete lines-of-sight in the reverse of the flight direction of ENVISAT, with tangent heights between 8 km and 68 km. The vertical resolution was ~ 3 km and the horizontal resolution was ~ 300 km along the line of sight. ENVISAT follows a sun-synchronous polar orbit, allowing MIPAS to sample globally, and to produce up to ~ 1000 atmospheric profiles per day. Coverage is quite uniform in latitude and time (see Fig. 4).

From the infrared spectra, ESA retrieved profiles of pressure, temperature, ozone, water vapour, HNO_3 , NO_2 , CH_4 and N_2O at up to 17 tangent points (ESA, 2004). MIPAS version 4.61 data, reprocessed offline, is used throughout this work, except in the ECMWF assimilation runs, where the Near Real Time v4.59 product was used. The differences between v4.59 and v4.61 processors are minor.

MIPAS ozone appears unbiased when compared to independent data except in the lower stratosphere where a small positive bias has been noted (Dethof, 2003a,b, 2004; Fischer and Oelhaf, 2004; Wargan et al., 2005; Geer et al., 2006). However, a comparison against ozonesondes using the MIPAS averaging kernels identified no bias (Migliorini et al., 2004). Using the analyses as a transfer standard, and treating MIPAS retrievals as point measurements, this intercomparison suggests a positive bias of order 5% in the upper stratosphere with respect to HALOE, increasing to roughly 10% with respect to sonde and HALOE in the lower stratosphere. The official MIPAS validation papers are currently in preparation.

To calculate statistics of (analysis – MIPAS), the analyses are interpolated from the intercomparison common grid to the MIPAS retrieval points. The paired differences are then binned to the nearest pressure level on the intercomparison grid. Tests showed that at the tropopause, the statistics had a sensitivity to the vertical interpolation method chosen, though elsewhere the results are robust no matter which method is used. The interpolation approach was chosen because it gives the smallest biases between MIPAS and independent data at the tropopause.

**Intercomparison of
ozone analyses**A. J. Geer et al.

Title Page

Abstract

Introduction

Conclusions

References

Tables

Figures

◀

▶

◀

▶

Back

Close

Full Screen / Esc

Printer-friendly Version

Interactive Discussion

The statistics are based on a set of MIPAS observations including all those supplied in the ESA data files, except those that fail a set of quality controls developed during data assimilation experiments at DARC (Lahoz et al., 2006). When assimilated, however, different sets of observations will have been used, depending upon the quality control applied in each system.

3.2 Ozonesondes

Ozonesondes are used as independent data to validate the analyses. Profiles have been obtained from the World Ozone and Ultraviolet Radiation Data Centre (WOUDC, <http://www.woudc.org/>), Southern Hemisphere Additional Ozonesondes project (SHADOZ, <http://croc.gsfc.nasa.gov/shadoz/>, Thompson et al., 2003a,b) and the Network for the Detection of Stratospheric Change (NDSC, <http://www.ndsc.ncep.noaa.gov/>). We use ozonesonde ascents from 42 locations, not including the Indian stations, and comprising mostly Electrochemical Concentration Cell (ECC) types, with five locations using Carbon-Iodide sondes and one location using Brewer-Mast sondes. We approach this dataset in the knowledge that it may be somewhat heterogeneous, both in the sonde types used, but also in the correction factors applied to the data, and in the operating procedures at each site. See Komhyr et al. (1995) and Thompson et al. (2003a) for more discussion of the importance of these techniques and procedures. However, we believe this heterogeneity is worth accepting in order to gain the widest global coverage. The number of sonde ascents available to this intercomparison, and their latitudinal and temporal coverage, are summarised in Fig. 5. Sondes typically make measurements from the surface to around the 10 hPa level.

Total error for ECC sondes is estimated to be within -7% to $+17\%$ in the upper troposphere, $\pm 5\%$ in the lower stratosphere up to 10 hPa and -14% to $+6\%$ at 4 hPa (Komhyr et al., 1995). Errors are higher in the presence of steep ozone gradients and where ozone amounts are low.

In order to compare sonde profiles, with a relatively high vertical resolution, to the analyses on the intercomparison common grid, the sonde profiles are averaged over a

Intercomparison of ozone analyses

A. J. Geer et al.

Title Page

Abstract

Introduction

Conclusions

References

Tables

Figures

◀

▶

◀

▶

Back

Close

Full Screen / Esc

Printer-friendly Version

Interactive Discussion

layer bounded by the half-way points (calculated linearly) between the common pressure levels. For example, analyses at 100 hPa are compared to the mean of any ozonesonde profile points between 125 hPa and 84 hPa. We disregard the horizontal movement of sondes and assign the measurement position as the launch longitude and latitude. Especially within the polar vortex, sondes may drift long distances during their ascent, but tracking information is not generally supplied for the sonde ascents used here.

Figure 6 gives an example of the intercomparison, showing both the full-resolution sonde profile and the layer-averages used to calculate statistics, alongside a number of different analyses. Most of these capture a small bulge in ozone between 200 and 300 hPa, but do not capture the full strength of what is likely a laminar intrusion of stratospheric air.

3.3 HALOE

HALOE (Russell et al., 1993) uses solar occultation to derive atmospheric constituent profiles. HALOE is used here as independent data for validation. Figure 7 shows the coverage available. The nature of the solar occultation technique makes the data sparse in time and space, with about 15 observations per day at each of two latitudes. The horizontal resolution is 495 km along the orbital track and the vertical resolution is about 2.5 km.

We use an updated version 19 product, screened for cloud using the algorithm of Hervig and McHugh (1999), and available from the HALOE website (<http://haloedata.larc.nasa.gov/>). We found that, compared to the previously available version 19, the one with cloud screening substantially improved the quality of results in this intercomparison around the tropical tropopause. Aside from the cloud screening, version 19 ozone retrievals are nearly identical to those of v18, and above the 120 hPa level they agree with ozonesonde data to within 10% (Bhatt et al., 1999). Below this level, profiles can be seriously affected by the presence of aerosols and cirrus clouds.

HALOE profiles are supplied on 271 levels with very close vertical spacing, but ver-

Intercomparison of ozone analyses

A. J. Geer et al.

Title Page

Abstract

Introduction

Conclusions

References

Tables

Figures

◀

▶

◀

▶

Back

Close

Full Screen / Esc

Printer-friendly Version

Interactive Discussion

tical variation is smooth due to the much broader vertical resolution of the instrument. Hence, to compare to the analyses on common pressure levels, HALOE is simply interpolated between the nearest two of the 271 levels. Longitudes and latitudes vary with height in HALOE profiles but for this comparison, those at 10 hPa are taken to be representative of all levels.

3.4 TOMS

The Total Ozone Mapping Spectrometer (TOMS) measures backscattered ultraviolet radiances with high horizontal resolution (38 km by 38 km) and daily near-global coverage. There are small gaps between orbital coverage bands near the equator. During the intercomparison period, due to the lack of sunlight at very high latitudes, there is no data in July, August and September in the southern high latitudes; the same for October and November in the north. TOMS is not assimilated in any of the analyses evaluated here.

We use version 8 of the level 3 total column ozone product, which is a daily composite of binned observations. Version 8 has partial corrections for calibration problems in the post-2000 TOMS data from the Earth Probe satellite, and improved retrievals under extreme conditions (high observation angles, in the Antarctic, aerosol loading) compared to v7 (McPeters, personal communication, 2004). A full validation of TOMS v8 has not yet been published, but v7 uncertainties were estimated as about 2% for the random errors, 3% for the absolute errors and somewhat more at high latitudes due to the higher zenith angle (McPeters et al., 1998).

4 Method

All analyses were interpolated from their native resolutions onto a common grid. The resolution of the common grid was determined by the need to minimise storage requirements whilst not losing important geophysical variability in time or space, and

Intercomparison of ozone analyses

A. J. Geer et al.

Title Page

Abstract

Introduction

Conclusions

References

Tables

Figures

◀

▶

◀

▶

Back

Close

Full Screen / Esc

Printer-friendly Version

Interactive Discussion

so minimising collocation error when comparing with independent data. Based on the results of sensitivity tests (Sect. 4.1), the choice of a 3.75° longitude by 2.5° latitude grid, 37 fixed pressure levels, and twice daily analyses (00Z and 12Z) appears to be a reasonable compromise. Pressure levels are 6 per decade between 0.1 hPa and 100 hPa (as used on the Upper Atmosphere Research Satellite (UARS) project). Below this, there are levels at 150, 200 hPa, and so on every 50 hPa down to 1000 hPa. All comparisons against independent data, except those against TOMS, were made using analyses on the common grid. In the case of TOMS, experiments showed that going from the 50 levels of the DARC analyses to the 37 common levels caused a bias in total column calculations of between 3 DU and 7 DU. Hence, ozone columns were calculated from analyses at their original vertical resolution. All vertical interpolations were done linearly in $\ln(P)$ (where P is pressure) and all horizontal interpolation, bilinearly in longitude and latitude.

Statistics were built up from the difference between analyses and observations. In this paper, statistics were binned in the regions referred to here as the southern and northern high latitudes (90° S to 60° S and 60° N to 90° N, respectively), the southern and northern midlatitudes (60° S to 30° S and 30° N to 60° N respectively) and the tropics (30° S to 30° N). Statistics were binned monthly; also for the entire period 18 August 2003 to 30 November 2003 (before 18 August 2003, the DARC analyses were not adequately spun up).

Ozone amounts vary by many orders of magnitude through the atmosphere. Units of partial pressure emphasise the UTLS; units of mixing ratio emphasise the mid and upper stratosphere. In order to give approximately equal weight through the atmosphere, statistics were normalised with respect to climatology, and displayed as a percentage. As an example, for a particular bin (e.g. July in the tropics at 100 hPa), where i runs over all n observations in this bin, the percentage mean difference d , between analysis interpolated to the observation positions (A_i) and observations (I_i), would be calculated

**Intercomparison of
ozone analyses**A. J. Geer et al.

[Title Page](#)[Abstract](#)[Introduction](#)[Conclusions](#)[References](#)[Tables](#)[Figures](#)[◀](#)[▶](#)[◀](#)[▶](#)[Back](#)[Close](#)[Full Screen / Esc](#)[Printer-friendly Version](#)[Interactive Discussion](#)

as

$$d = 100 \times \frac{\frac{1}{n} \sum_i (A_i - I_i)}{c}, \quad (1)$$

where c is the mean of the Logan/Fortuin/Kelder climatology at this level, for this month, and for this region (e.g. the tropics, 30° S to 30° N). This climatology does not go above 0.3 hPa, so at the top levels (0.21, 0.15 and 0.1 hPa) we use mean ozone from the BASCOE v3q33 run instead. This particular approach to normalisation was chosen to reduce the influence of very small ozone amounts on the percentage statistics. If a formulation is chosen that includes I_i in the denominator, d can show very large percentage values at the tropical tropopause and in the ozone hole.

4.1 Sensitivity tests

We investigated the effect of the horizontal and temporal grid resolution on the statistics of $(A_i - I_i)$, by varying the time and space resolution of the ECMWF and DARC analyses in comparisons to independent data. As previously described, the intercomparison only considers analyses at 00Z and 12Z; hence independent data collocations are found within a time window of 12 h. We found that changing the spatial or temporal resolution of the common grid had very little effect on the mean differences between analysis and sonde. However, the standard deviations were affected in some regions and Fig. 8 shows results for four selected time windows: 6, 12, 24 and 48 h. We first consider the tropical stratosphere (Fig. 8a), where changing the temporal and horizontal resolution makes very little difference, and the horizontal and temporal variability of ozone appears to be fairly small. The main regions where the temporal and spatial resolution are important are the polar stratosphere (e.g. Fig. 8b) and the midlatitude UTLS (e.g. Fig. 8c). Here, time windows longer than 12 h appear to increase standard deviations quite considerably. Increased spatial resolution is unimportant in the polar regions, but does have a small effect in the UTLS. Degrading spatial resolution further to that of the BASCOE analyses (5° by 3.75°) made essentially no difference, and the

Intercomparison of ozone analyses

A. J. Geer et al.

Title Page

Abstract

Introduction

Conclusions

References

Tables

Figures

◀

▶

◀

▶

Back

Close

Full Screen / Esc

Printer-friendly Version

Interactive Discussion

results are not shown. For the intercomparison, the 12 h time window and 3.75° by 2.5° grid appear a reasonable compromise.

In the mesosphere, there is a strong diurnal cycle in ozone (Sect. 5.5). Figure 9 examines the effect of this on the statistics of (BASCOE – HALOE) ozone for the tropical region. Results at other latitudes are similar. Only the BASCOE analyses simulate a diurnal cycle. In a special run of the assimilation system, profiles were generated at HALOE observation locations at the nearest model timestep, giving a maximum time mismatch of 15 min. Statistics generated using a 12 h time window are substantially different above 0.5 hPa, indicating the effect of the diurnal cycle. Hence in this work we do not show MIPAS or HALOE statistics above the 0.5 hPa level.

5 Results

This section first gives an overview of the results of the intercomparison, by examining statistics for the period 18 August 2003 to 30 November 2003. We first look at mean differences compared to ozonesonde, HALOE and MIPAS (Sect. 5.1), then the standard deviations of these differences (Sect. 5.2). We examine MIPAS calibration using the analyses as a transfer standard (Sect. 5.3) and compare the analyses to TOMS (Sect. 5.4). Through most of the stratosphere, the analyses compare well to independent data, but there are problems in the stratospheric polar vortex, at the stratopause and in the mesosphere, in the troposphere, in the extratropical UTLS, and at the tropical tropopause. A number of these regions are examined in more detail in Sects. 5.5, 5.6 and 5.7.

5.1 Biases

Figures 10, 11 and 12 show respectively the biases against HALOE, sonde and MIPAS, normalised by climatology (see Sect. 4). Indicated at the top of the figure is the number of profiles on which the statistics are based. Statistics are only plotted at a particular

Intercomparison of ozone analyses

A. J. Geer et al.

Title Page

Abstract

Introduction

Conclusions

References

Tables

Figures

◀

▶

◀

▶

Back

Close

Full Screen / Esc

Printer-friendly Version

Interactive Discussion

level if the number of collocations with data available is 50% (25% for MIPAS) of the total number of profiles. For example, less than half of sonde ascents reach the 10 hPa level in the northern hemisphere (NH) high latitudes in Fig. 11, so to avoid unrepresentative results, this level is not plotted. Comparisons are not done above 0.5 hPa, because of the diurnal cycle in ozone.

For most of the stratosphere and mesosphere above 50 hPa, biases between the analyses and HALOE, sonde and MIPAS are between -10% and 10%. The ECMWF, DARC, and KNMI TEMIS analyses have larger biases in the upper stratosphere and mesosphere. DARC analyses have a positive bias which rises to 40% at 0.5 hPa. The bias is uniform at all latitudes and, by examination of the monthly statistics (not shown), uniform in time. KNMI TEMIS analyses have a uniform negative bias, growing to -40% at 0.5 hPa. Section 5.5 shows that the KNMI TEMIS and DARC biases result from the linear chemistry schemes used in the models. The ECMWF bias is smaller, and has not been attributed, but again the linear chemistry scheme is the most likely explanation.

In the lower stratosphere (LS, 100 hPa to 50 hPa), analyses are biased typically 10% high compared to sonde and HALOE, but reaching 50% at 100 hPa in the tropics. Biases are typically smaller against MIPAS, reflecting a small (~10%) positive bias between MIPAS and the independent data at these levels (Sect. 5.3). There are big variations between different analyses in the lower stratosphere in the SH high latitudes and near the tropical tropopause. These variations are examined in Sects. 5.6 and 5.7, respectively.

At SH high latitudes, KNMI TEMIS analyses stand out with a positive bias of 10 to 15% between 10 hPa and 30 hPa against MIPAS, HALOE and sonde. Above and below this level, the bias becomes negative. There is a ~60% negative bias against sonde at 200 hPa. The KNMI TEMIS analyses are based only on total column observations; the vertical profile is model-determined. To get a better vertical profile would require either model improvements or the assimilation of profile data (e.g., Struthers et al., 2002).

The Juckes analyses are essentially unbiased when compared to MIPAS observations assimilated on isentropic levels (Juckes, 2005), yet biases exist when compared

Intercomparison of ozone analyses

A. J. Geer et al.

Title Page

Abstract

Introduction

Conclusions

References

Tables

Figures

◀

▶

◀

▶

Back

Close

Full Screen / Esc

Printer-friendly Version

Interactive Discussion

**Intercomparison of
ozone analyses**

A. J. Geer et al.

Title Page

Abstract

Introduction

Conclusions

References

Tables

Figures

◀

▶

◀

▶

Back

Close

Full Screen / Esc

Printer-friendly Version

Interactive Discussion

to MIPAS on pressure levels in Fig. 12. These are likely explained by biases (e.g., De-
thof, 2004) between the MIPAS temperatures used to assimilate the data on isentropic
levels, and the ECMWF temperatures used here in the vertical transformation to pres-
sure levels. This bias results in a small vertical uncertainty in the pressure assignment
of both the Jukes and MIMOSA ozone profiles.

In the troposphere (below 100 hPa), some analyses show quite substantial biases
when compared to sonde (Fig. 11). BASCOE analyses have a negative bias of typ-
ically 50% at all latitudes. DARC analyses have a large positive bias in the SH near
the ground, associated with the Cariolle v1.0 scheme. MOCAGE-PALM Cariolle v2.1
analyses have a positive bias, particularly in the tropics, and this is known to be a
problem with v2.1 of the Cariolle scheme. There are no ozone profile observations
below ~400 hPa in any of the analyses, though the ECMWF system assimilates total
columns from GOME and partial columns from SBUV. None of the models represent
detailed tropospheric chemistry. However, the MOCAGE-PALM Reprobus run does
include upper-tropospheric chemistry. These analyses are quite successful in minimis-
ing bias against ozonesonde, as are the ECMWF analyses, excluding the lowermost
tropical troposphere. KNMI TEMIS analyses are also relatively successful; they simply
impose a relaxation to tropospheric climatology. In general, the most likely explanation
for the tropospheric biases is limitations in the ozone chemistry schemes used in the
other models, on top of a lack of observational data.

Next we examine biases in the KNMI SCIAMACHY profile analyses. SCIAMACHY
profiles were only available in quantity for assimilation for October and November dur-
ing the intercomparison period. November analysis biases against sonde are shown
in Fig. 13; October biases are similar, as are the results against HALOE and MIPAS.
In the NH in the lower stratosphere (200 to 10 hPa), the SCIAMACHY profile analyses
have up to 20% negative bias compared to sonde and are notably different from the
other analyses. This is thought to be due to problems with the shape of the SCIA-
MACHY profiles in the lower stratosphere. However, the SH stratosphere shows only
small biases. The troposphere also shows small biases against sonde, outside of the

SH high latitudes. SCIAMACHY profiles do not go below ~12 km, thus this is due to the relaxation of the photochemical scheme towards Fortuin and Kelder (1998) climatology. Against HALOE and MIPAS (figures not shown) biases are no more than +20% in the upper stratosphere and mesosphere, which is comparable in magnitude to many of the other analyses (Figs. 10 and 12).

5.2 Standard deviations

Figures 14, 15 and 16 show the standard deviations of differences between analyses and HALOE, sonde and MIPAS ozone respectively, normalised against climatology (see Sect. 4). As a reference point, these figures also show the standard deviations of the differences between observations and the Logan/Fortuin/Kelder climatology. Again, statistics are only plotted at a particular level if the number of collocations is 50% (25% in the case of MIPAS) of the total number of profiles available.

Analyses demonstrate smaller standard deviations than climatology throughout the high latitude stratosphere, and in the midlatitude lower stratosphere and upper troposphere (10 hPa to 300 hPa). In other regions, particularly the tropical stratosphere, analyses do little better, or even worse, than climatology. These are regions of relatively low synoptic variability, and in the upper stratosphere, ozone is close to photochemical equilibrium. By contrast, at high latitudes in the stratosphere, ozone transport is important and there is strong synoptic variability. Looking at the monthly statistics (not shown), the analyses demonstrate the largest improvements over climatology at high latitudes in September, October and November. In the SH, there is strong synoptic variability due to the onset of the top-down breakup of the polar vortex (e.g., Lahoz et al., 2006). In the NH, synoptic variability is likely associated with increasing surf-zone activity around the developing vortex during these months. The midlatitude UTLS is also a region of high variability in ozone. Ozone has strong gradients across the tropopause; in data assimilation systems these gradients are expected to provide dynamical information, particularly on the horizontal position of the polar front (e.g., Riishøjgaard, 1996; Peuch et al., 2000; Hudson et al., 2003).

Intercomparison of ozone analyses

A. J. Geer et al.

Title Page

Abstract

Introduction

Conclusions

References

Tables

Figures

◀

▶

◀

▶

Back

Close

Full Screen / Esc

Printer-friendly Version

Interactive Discussion

**Intercomparison of
ozone analyses**A. J. Geer et al.

Title Page

Abstract

Introduction

Conclusions

References

Tables

Figures

◀

▶

◀

▶

Back

Close

Full Screen / Esc

Printer-friendly Version

Interactive Discussion

In the mid and upper stratosphere (above 50 hPa), standard deviations are typically less than 10% against HALOE and (to 10 hPa only) sonde data. However, there are some exceptions. DARC analyses are worse above the 1 hPa level; this is likely due to problems with the linear photochemistry scheme. ECMWF analyses have relatively high standard deviations (15%) versus HALOE in the SH high latitudes, between 10 hPa and 1 hPa. This may be associated with the ozone photochemistry scheme, or it could be due to known problems in ECMWF upper stratospheric temperatures at high latitudes (Randel et al., 2004). Standard deviations of the DARC and ECMWF analyses against MIPAS are also larger compared to the other analyses in the upper stratosphere, supporting the conclusions drawn from HALOE, and suggesting that the model is dominating over the MIPAS observations. KNMI TEMIS analyses also show relatively large standard deviations against MIPAS in the high latitude upper stratosphere, compared to the other analyses, but this might be expected since these are the only analyses in which MIPAS is not assimilated.

In the lower stratosphere (between 50 hPa and 100 hPa), standard deviations against sonde, HALOE and MIPAS become larger than in the upper stratosphere. In the mid-latitude comparisons (30° S to 60° S and 30° N to 60° N) analyses show standard deviations against MIPAS, HALOE and sonde, of ~20% at 100 hPa. At high latitudes and in the tropics, standard deviations are larger. At 100 hPa in the tropics, there is disagreement between the data types. The standard deviations of (analysis – sonde) are ~30%, compared to ~85% for MIPAS and ~70% for HALOE. This suggests a large degradation in the quality of the satellite retrievals at these levels, which is likely due to the effects of undetected cloud, as well as the sharp vertical gradients in temperature and ozone. The degradation in quality of HALOE retrievals at 100 hPa is already well-known (e.g., Bhatt et al., 1999). Section 5.3 investigates MIPAS data quality further. At the tropical tropopause and in the SH high latitude lower stratosphere, compared to sonde, there are notable differences between the analyses themselves. These are examined in more detail in Sects. 5.6 and 5.7.

In the troposphere, standard deviations of (analysis – sonde) range between 10%

and 80% (Fig. 15). None of the analyses does better than climatology at levels below 400 hPa; above this level the analyses do demonstrate improvements over climatology. DARC and ECMWF analyses show large standard deviations in the SH. The explanation for the high standard deviations in the troposphere is likely the same as for the large biases: no ozone profile information is assimilated below 400 hPa and the ozone photochemistry schemes do not simulate tropospheric chemistry well. KNMI TEMIS analyses do relatively well in the troposphere with a simple relaxation to climatology.

5.3 MIPAS validation

Previous sections have indicated differences in ozone amounts between MIPAS, ozonesonde and HALOE. Using the analyses as a transfer standard, we can examine the bias between MIPAS and independent data. This has the advantage, compared to colocating pairs of observations, that all available observations are included in the sample. Note that in all comparisons here, MIPAS data are treated as point retrievals and the analyses are interpolated to the MIPAS retrieval points linearly in $\ln(P)$ in the vertical. It is well known that comparison in terms of radiances, or the use of averaging kernels (Rodgers, 2000; Migliorini et al., 2004), produces a better representation of the information content of the retrievals; these methods are increasingly used in calibration and validation activities. But here, no assimilation system uses MIPAS radiances or an averaging kernel representation (both the subject of much ongoing research), so it is the bias in MIPAS retrievals, treated as a point values, that is important.

The bias between MIPAS and sonde can be estimated from the statistics shown in Figs. 10, 11 and 12 as, for example, $(\text{MIPAS} - \text{sonde}) = (\text{MIPAS} - \text{analysis}) - (\text{sonde} - \text{analysis})$. Figure 17 summarises the biases calculated using BASCOE v3q33 analyses as the transfer standard. These are chosen for their small standard deviations against independent data through the stratosphere (Figs. 14 and 15), though Fig. 17 would in general be similar no matter which analyses are chosen (figures not shown). The sampling patterns of sonde and HALOE vary with time (Figs. 5 and 7) and the biases show some variation when broken down by month, but the features identified in Fig. 17

Intercomparison of ozone analyses

A. J. Geer et al.

Title Page

Abstract

Introduction

Conclusions

References

Tables

Figures

◀

▶

◀

▶

Back

Close

Full Screen / Esc

Printer-friendly Version

Interactive Discussion

are broadly typical of the period.

In the upper stratosphere (above ~ 30 hPa), MIPAS measures approximately 5% more ozone than HALOE. In the lower stratosphere (100 to 30 hPa), MIPAS has a high bias of typically 10% compared to sonde and HALOE. Excepting Migliorini et al. (2004), this lower stratospheric bias is a consistent feature of other studies that have considered the calibration of MIPAS for a variety of periods and data versions (Dethof, 2003a,b, 2004; Fischer and Oelhaf, 2004; Wargan et al., 2005; Geer et al., 2006).

At 100 hPa in the tropics and midlatitudes, MIPAS appears unbiased against HALOE and sonde. However, if statistics are calculated by interpolating from MIPAS retrieval points to the intercomparison fixed pressure levels, biases at 100 hPa are +20% in the midlatitudes and +50% in the tropics (figures not shown). The fixed pressure levels are more closely spaced than the MIPAS retrievals. Because, particularly at the tropical tropopause, there is a sharp transition between very low tropospheric ozone values and much higher stratospheric ones, interpolation tends to increase the ozone amounts. Also noting that previous studies do not provide consistent conclusions on the biases at 100 hPa in the tropics and midlatitudes, the results should here be treated with caution. Elsewhere in the stratosphere, however, the biases are essentially insensitive to the vertical interpolation strategy. Standard deviations also appear mostly insensitive to interpolation strategy at 100 hPa and above.

At 200 hPa, the high bias against HALOE is likely a problem with HALOE observations. Biases between MIPAS and sonde below 100 hPa are relatively small, except in the SH at 300 hPa, though again a sensitivity to the interpolation strategy mean these results should be treated with caution.

Finally, we examine the fact that standard deviations between MIPAS and analyses are in some cases much larger than between sonde and analyses. Section 5.2 noted that, at the tropical tropopause, MIPAS standard deviations are $\sim 85\%$, compared to $\sim 30\%$ for sonde. The MIPAS and sonde sampling patterns are quite different (Figs. 4 and 5). Ozonesondes are concentrated just south of the equator for the SHADOZ project; MIPAS samples relatively uniformly with latitude. Looking at just the region

Intercomparison of ozone analyses

A. J. Geer et al.

Title Page

Abstract

Introduction

Conclusions

References

Tables

Figures

◀

▶

◀

▶

Back

Close

Full Screen / Esc

Printer-friendly Version

Interactive Discussion

between 10°S and the equator, we can get a similar sampling pattern for the two instrument types. Using just this latitude band, Fig. 18 confirms the general conclusions of Sect. 5.2: at 100 hPa, against sonde, standard deviations are relatively small (15% to 35%); against MIPAS, relatively large (~95%). These results are largely unaffected by the choice of vertical interpolation strategy for calculating the statistics. It appears that as for HALOE, observation quality degrades at these levels. In addition to the difficulties of identifying the sharp ozone boundary at the tropical tropopause using an instrument with a ~3 km vertical resolution, the observations could also be affected by undetected high cloud (e.g., Dethof, 2003b).

5.4 TOMS

Total column ozone observations are sensitive to ozone predominantly in the lower stratosphere, with a smaller contribution from the troposphere. In mean terms, BASCOE and KNMI TEMIS analyses are closest to TOMS total columns (Fig. 19). The other analyses show typically 20 to 40 DU positive biases against TOMS, consistent with the typically positive biases seen against sonde and HALOE in the lower stratosphere, particularly (by examination of the monthly statistics) in September, October and November in the ozone hole region. The BASCOE analyses have a similar positive bias in the lower stratosphere, but a negative bias in the troposphere (Fig. 11) contributes to closer agreement with TOMS. The good agreement between KNMI TEMIS analyses and TOMS probably reflects good agreement between TOMS and the assimilated total columns from SCIAMACHY. However, this does not say anything about the KNMI TEMIS ozone profiles: in fact a small negative bias against ozonesonde at around 200 hPa helps balance positive biases in the lower stratosphere (Fig. 11).

In terms of standard deviation (Fig. 20), there is little to separate the analyses, with magnitudes typically 10 DU to 20 DU. The ECMWF operational analyses stand out, but they were assimilating only SBUV and very limited GOME observations during August and September. KNMI TEMIS analyses have the lowest standard deviations, as again would be expected due to the assimilation of SCIAMACHY columns. The correlation

Intercomparison of ozone analyses

A. J. Geer et al.

Title Page

Abstract

Introduction

Conclusions

References

Tables

Figures

◀

▶

◀

▶

Back

Close

Full Screen / Esc

Printer-friendly Version

Interactive Discussion

coefficient (e.g., [Spiegel and Stephens, 1999](#)) between analysis and TOMS, calculated from samples in 5° latitude bands, reveals wider differences between analyses in the tropics (Fig. 21).

The time evolution of the standard deviation (Fig. 22) reveals a ~10 day spinup at the beginning of July in the MOCAGE-PALM runs, and a similar spinup in the DARC analyses. These were started on 4 August; standard deviations against TOMS decline until about 14 August. This length of spinup is expected in the DARC system and is longest in the lower stratosphere ([Geer et al., 2006](#)). The other analyses are sections of longer runs that were started well before July; hence no spinup is seen. The ECMWF operational analyses show particularly large standard deviations through August and September, when GOME observations were very limited. Smaller standard deviations are seen when MIPAS are assimilated (throughout the ECMWF MIPAS run, and after 7 October in the ECMWF operational analyses). This shows that the assimilation of MIPAS data substantially improved the ECMWF analyses. See [Dethof \(2003a\)](#) for more details.

Figure 22 also includes statistics for the KNMI SCIAMACHY profile analyses. These are largely based on the free running model before October. In September standard deviations of ~25 DU are comparable those from the ECMWF operational analyses. However, in October and November, assimilation of SCIAMACHY profiles does not reduce the standard deviations to the ~15 DU level of the other analyses. This is in contrast to the ECMWF analyses, which improve markedly when MIPAS observations are assimilated.

Standard deviations and correlations with TOMS can be improved by substituting the [Logan \(1999\)](#) climatology into the analyses at 200 hPa and below. Figure 23 shows that for the ECMWF, MOCAGE-PALM, BASCOE and DARC analyses, correlations become substantially larger between 20° S and 10° N compared to when the analyses are used throughout the atmosphere (Fig. 21). Examination of the column fields (not shown) reveals that the analyses typically lack structure in the equatorial total column ozone field. When the Logan climatology is substituted in the troposphere, the combination

Intercomparison of ozone analyses

A. J. Geer et al.

[Title Page](#)[Abstract](#)[Introduction](#)[Conclusions](#)[References](#)[Tables](#)[Figures](#)[◀](#)[▶](#)[◀](#)[▶](#)[Back](#)[Close](#)[Full Screen / Esc](#)[Printer-friendly Version](#)[Interactive Discussion](#)

of tropospheric climatology and stratospheric analyses appears to give a better representation the zonal tropical “wave-1” pattern in total column ozone (Thompson et al., 2003b), which is due to zonal variations in tropospheric ozone. It could be argued that since the Logan (1999) analyses are partly based on TOMS tropospheric residuals, improved agreement with TOMS fields might be expected. It is also possible that the tropical variability of TOMS columns may be affected by high clouds. Nevertheless, Thompson et al. (2003b) have confirmed the tropospheric zonal “wave-1” using independent ozonesonde data.

5.5 Upper stratosphere and mesosphere

In the upper stratosphere and mesosphere, discrepancies between analyses, and between analyses and independent data, can be explained in terms of the modelled ozone photochemistry. In these regions, ozone is close to photochemical equilibrium, and above ~0.5 hPa, there is a diurnal cycle in ozone that is only represented in the BASCOE analyses, which include detailed chemistry. Comparing to HALOE ozone with a maximum time mismatch of 15 min (Fig. 9) shows that the BASCOE analyses produce a good representation of ozone at these levels.

Figure 24 shows examples of analysed ozone fields in the mesosphere. DARC and KNMI analyses are not shown in this figure because of their large biases at these levels (Fig. 10). Linear photochemistry schemes, as used in ECMWF analyses, are daily averaged and do not have a diurnal cycle. Hence, ECMWF produces a relatively uniform ozone field. The Juckes analyses, which do not include modelled ozone chemistry, show stripes caused by the diurnal sampling of the MIPAS ascending and descending orbits. However, at levels below 0.5 hPa where the diurnal cycle is not important, the Juckes analyses are typically as close to HALOE as the BASCOE analyses (standard deviations <10%, Fig. 14).

Biases in the KNMI TEMIS and DARC analyses above 5 hPa can be explained by the linear ozone photochemistry schemes employed. In the DARC analyses presented here, though not in those of Geer et al. (2006), the radiation term of the Cariolle scheme

Intercomparison of ozone analyses

A. J. Geer et al.

Title Page

Abstract

Introduction

Conclusions

References

Tables

Figures

◀

▶

◀

▶

Back

Close

Full Screen / Esc

Printer-friendly Version

Interactive Discussion

(Cariolle and Déqué, 1986) was incorrectly implemented, leading to a discrepancy between analysed overhead column ozone and the scheme's internal climatology, giving a positive forcing in ozone. This problem was identified and the month of October re-run with (a) a correctly implemented Cariolle scheme and (b) the LINOZ scheme (McLinden et al., 2000), as used in the KNMI TEMIS analyses. Figure 25 shows the bias against MIPAS in these October runs. We note that MIPAS is not independent data, but it offers a much better coverage than HALOE for the month of October (Figs. 4 and 7) and that MIPAS and HALOE are biased by no more than ~5% with respect to each other at these levels (Sect. 5.3). Figure 25 confirms that the DARC biases were due to an incorrect implementation of the Cariolle scheme, which produced excessive ozone in the upper stratosphere and mesosphere. It is also clear that the LINOZ scheme causes an excessive reduction in upper stratospheric and mesospheric ozone, explaining the bias in the KNMI TEMIS analyses. McCormack et al. (2004) have already identified these problems with LINOZ. The results of the DARC study of Cariolle schemes will be described in more detail in a future paper.

The BASCOE analyses also illustrate the sensitivity of ozone amounts at these levels to the modelled ozone photochemistry. In the v3d24 analyses, the O₂ photolysis rate was multiplied by 1.25 to gain better agreement with MIPAS. In the newer v3q33 version of BASCOE, this scaling factor was removed. Figures 10 and 12 show that, compared to MIPAS and HALOE, BASCOE v3q33 analyses have less ozone than v3d24 throughout the upper stratosphere and mesosphere (above 10 hPa). The difference peaks at 15% at 0.5 hPa; here the v3d24 analyses are closer to MIPAS and the v3d33 analyses are closer to HALOE.

5.6 Ozone hole

At high latitudes in the southern hemisphere, at levels between 100 hPa and 50 hPa, there are variations in the performance of the analyses, which in general overestimate the ozone amount, and have standard deviations of up to 20% against ozonesonde. These discrepancies come mostly during the later part of the intercomparison period,

Intercomparison of ozone analyses

A. J. Geer et al.

Title Page

Abstract

Introduction

Conclusions

References

Tables

Figures

◀

▶

◀

▶

Back

Close

Full Screen / Esc

Printer-friendly Version

Interactive Discussion

between September and November, and can be explained by the analyses' ability to capture the development of the ozone hole. Apart from KNMI, who assimilate SCIAMACHY, and ECMWF who assimilated MIPAS v4.59 alongside GOME and SBUV, all other analyses assimilate only MIPAS v4.61, so any differences between them must be due to differences either in the models or in the use of the observations.

Figures 26, 27 and 28 show the time evolution of analysed ozone over the South Pole compared to sonde observations at 32 hPa, 46 hPa and 68 hPa respectively. Figure 1 shows the situation at 68 hPa on 31 August 2005, with ozone depletion already under way in a ring around the South Pole, in regions where sunlight has returned after the winter. At the South Pole itself, ozone depletion began at around 5 September, progressing to almost complete ozone destruction by early October (e.g. Fig. 27). In November 2003, the vortex was periodically displaced off the pole by growing anticyclones, but the lower stratosphere vortex (~100 hPa to ~50 hPa) itself remained relatively intact until December (Lahoz et al., 2006). In general, the analyses capture the rapid, early ozone depletion quite well, but few are able to achieve complete ozone destruction in October. The periodic vortex displacements of November are captured well at 32 hPa and 46 hPa but not at 68 hPa, where most analyses show an increase in ozone that is not observed in the sonde record.

MOCAGE-PALM Cariolle v2.1 analyses, and ECMWF (using v1.2 of the Cariolle scheme), capture the near-complete ozone destruction in October using a simple parametrization of heterogeneous ozone depletion. Both v1.2 and v2.1 of the Cariolle scheme have a term which is activated in sunlight below 195K (e.g., Dethof and Hólm, 2004). In the MOCAGE-PALM Cariolle v2.1 analyses, it was found that this term should not be switched on before the sun reaches a zenith angle of 87°. An earlier version of the MOCAGE-PALM Cariolle v2.1 analyses (not shown) instead used a zenith angle of 94° which gave erroneous early ozone depletion in September at 32 hPa, 20 hPa and 10 hPa. This early ozone depletion was also thought to be influenced by a possible low bias in ARPEGE temperatures, and the fact that MIPAS data are not assimilated beyond 80° S, meaning the ozone field is less constrained by observations there.

**Intercomparison of
ozone analyses**A. J. Geer et al.

Title Page

Abstract

Introduction

Conclusions

References

Tables

Figures

◀

▶

◀

▶

Back

Close

Full Screen / Esc

Printer-friendly Version

Interactive Discussion

**Intercomparison of
ozone analyses**A. J. Geer et al.

Title Page

Abstract

Introduction

Conclusions

References

Tables

Figures

◀

▶

◀

▶

Back

Close

Full Screen / Esc

Printer-friendly Version

Interactive Discussion

MOCAGE-PALM Reprobus and BASCOE v3d24 analyses each use detailed descriptions of heterogeneous chemistry. The Reprobus analyses achieve a good description of the full ozone destruction. In contrast, in the BASCOE v3d24 analyses, 1 to 2 ppmm of ozone remain through October at 46 hPa and 68 hPa. These analyses used a detailed heterogeneous chemistry scheme in the polar vortex and the PSCBox microphysics scheme (Larsen et al., 2000). This microphysics scheme has proven its validity in Arctic (Larsen et al., 2002, 2004) and Antarctic (Hoepfner et al., 2006) winters. However, PSCBox is sensitive to various input parameters, most importantly to the temperature. Gobiet et al. (2005) report considerable temperature biases (−2.5 to 3.5 K in zonal mean) in the ECMWF analyses (used to drive the BASCOE CTM) in the Antarctic polar vortex during the 2003 winter. Hoepfner et al. (2006) illustrate the sensitivity of PSCBox to temperature. Bias-corrections of ECMWF temperature should improve chlorine activation and denitrification, and the ozone hole representation in BASCOE v3d24. In a newer version of BASCOE, v3q33, the microphysics scheme was replaced by a parametrization which appears to be less sensitive to the temperature biases, and this achieves a more complete destruction of ozone in October.

DARC and KNMI TEMIS analyses each use a cold tracer formulation for heterogeneous ozone depletion (Eskes et al., 2003). Neither analysis shows ozone depletion to lower than ~0.5 ppmm at 68 hPa, and this is reflected in a general overestimation compared to ozonesonde in the SH high latitudes (see Fig. 11). DARC use Cariolle v1.0 photochemistry and this produces excessive ozone in the ozone hole (Geer et al., 2006). If Cariolle v2.1 photochemistry is used instead (experiments not shown here), the correct full ozone depletion is produced. KNMI TEMIS analyses use the LINOZ photochemistry scheme, which does not produce excessive ozone in the ozone hole, and so it is not clear why ozone amounts are not depleted further.

The Juckes and MIMOSA isentropic analyses include no modelled ozone chemistry. In the Juckes analyses, 1 to 2 ppmm of ozone remain through October at 46 hPa and 68 hPa. The ~10% positive bias in MIPAS at these levels, as compared to ozonesonde (Sect. 5.3), may be a partial explanation for the problem. The MIMOSA analyses

show several spikes of high ozone through October at 68 hPa, though not at 46 hPa or 100 hPa (not shown). At 68 hPa, MIMOSA ozone fields are very noisy within the ozone hole; Fig. 28 reflects the advection of patches of high and low ozone over the South pole in the analyses during October.

5 The rapid increase of ozone in November at 68 hPa in all analyses except KNMI TEMIS is contrary to sonde observations of continuing low ozone values (Fig. 28), yet is seen throughout the vortex in the analysis fields (no figures shown). The KNMI TEMIS analyses instead maintain a sharp gradient at the vortex edge and almost complete ozone depletion within, in common with ozonesonde observations. The others show
10 an ozone hole that both shrinks and fills in at these levels, in common with the MIPAS observations (figure not shown). An explanation would be the ~ 3 km vertical resolution of MIPAS. It is likely that either the vertical resolution, or vertical interpolation of MIPAS, is smearing information from higher levels down to the 68 hPa level. At 46 hPa, a similar rapid increase is confirmed in both analyses, ozonesonde (Fig. 27), and MIPAS (not
15 shown), as the vortex breaks down at these levels.

5.7 Tropical tropopause

At the tropical tropopause, there is a wide variation between analyses. In general, standard deviations against ozonesonde are relatively high (30% at 100 hPa) and few analyses do much better than zonal mean climatology (Fig. 15). There are positive biases
20 compared to sonde at 100 hPa between 30° S and 30° N in the MOCAGE-PALM Carille v2.1, MIMOSA and DARC analyses (Fig. 11). In contrast, ECMWF ozone amounts are 10% lower than sonde at 100 hPa. KNMI TEMIS, BASCOE and MOCAGE-PALM Reprobis are approximately consistent with sonde.

25 The principal factors that will influence ozone analyses at the tropical tropopause are the assimilated observations, the model's ability to transport ozone correctly, and the ozone background error covariance matrix. The vertical ozone gradient is very large in the UTLS, so variability in the ozone field can come through vertical advection, which could be due either to large-scale motion or convective activity. Ozone photochem-

Intercomparison of ozone analyses

A. J. Geer et al.

Title Page

Abstract

Introduction

Conclusions

References

Tables

Figures

◀

▶

◀

▶

Back

Close

Full Screen / Esc

Printer-friendly Version

Interactive Discussion

ical relaxation times are ~ 100 days in this region (e.g., [Cariolle and Déqué, 1986](#)), so chemistry should be unimportant, but contradicting this, differences are seen here between the two MOCAGE-PALM analyses.

Figure 29 shows examples of the analysis fields at 100 hPa on 17 October 2003.

5 Through most of the tropics, ozone amounts appear generally uniform and very low. The positive biases of the MOCAGE-PALM Cariolle v2.1, MIMOSA and DARC analyses are obvious by comparison to the other analyses. At the edge of the tropics, there is a transition to the higher ozone values of the surf-zone (see e.g., [Plumb, 2002](#)).

10 Figure 18 shows that between 10° S and the equator, the ECMWF MIPAS analyses and zonal mean climatology have the closest agreement to ozonesonde, with standard deviations of 15%. From Fig. 29 it appears that this good agreement with sonde is associated with a very uniform ozone field around the equator at 100 hPa. Other analyses show larger standard deviations of difference against ozonesonde, because they have much more ozone variability in the tropics. Based on the comparison with sondes, this variability is unlikely to be real. The zonal invariance of the equatorial UTLS ozone field is examined in more detail by [Thompson et al. \(2003a\)](#), see their Fig. 12).

There are a number of plausible explanations for the problems in the analyses; it is likely that the explanations may be different in different systems. MIPAS ozone is of poorer quality at 100 hPa in the tropics, showing excessive noise (Fig. 18). It is also well-known that tropical wind fields in assimilated datasets are poorly represented (e.g., [Žagar, 2004](#)). When used to transport stratospheric tracers, they produce excessive horizontal mixing between the the tropics and the extratropics, and excessive vertical mixing between the UTLS and higher levels in the stratosphere (e.g., [Schoeberl et al., 2003](#); [Tan et al., 2004](#)).

25 In the case of the ECMWF analyses, Fig. 2 suggests that MIPAS data have very little impact on the ozone distribution at 100 hPa in the tropics. Hence, the smooth field is indicative of good quality transport. In CTM studies, the ECMWF 4D-Var operational analyses have been seen to produce better age-of-air values, i.e. better stratospheric transport and mixing, than earlier 3D-Var analyses such as ERA-40 (e.g., [Scheele](#)

Intercomparison of ozone analyses

A. J. Geer et al.

[Title Page](#)[Abstract](#)[Introduction](#)[Conclusions](#)[References](#)[Tables](#)[Figures](#)[◀](#)[▶](#)[◀](#)[▶](#)[Back](#)[Close](#)[Full Screen / Esc](#)[Printer-friendly Version](#)[Interactive Discussion](#)

et al., 2005). However, ozone amounts are 10 to 20% lower than sonde at 100 hPa and 68 hPa (see Fig. 11); this may be due to continuing excessively fast transport from the troposphere.

The KNMI TEMIS, MIMOSA and BASCOE analyses are driven by ECMWF operational winds, so it might be expected that they also would produce smooth ozone fields. Instead they still show excessive structure in the tropics. A possible explanation (e.g., Stohl et al., 2004) may be the use of 6-hourly (3-hourly in the case of KNMI SCIAMACHY profile analyses) snapshots of the winds in the CTMs, as compared to the winds within the ECMWF model which evolve every timestep. Figure 2 suggests that compared to the rest of the stratosphere, BASCOE ozone is model-dominated at 100 hPa; hence transport is most likely the cause, but noisy MIPAS observations may also be responsible for some of the tropical variability.

The KNMI SCIAMACHY profile assimilation ozone field is smoother than the KNMI TEMIS total column analyses in Fig. 29. The MOCAGE-PALM Reprobus analyses are smoother than the MOCAGE-PALM Cariolle v2.1 analyses. This smoothness in both cases results in smaller standard deviations with respect to sonde (Fig. 18 and similar comparisons for the SCIAMACHY profile analyses, not included this paper.) In the case of the MOCAGE-PALM analyses, the inclusion of upper-tropospheric chemistry in the Reprobus runs does appear to improve the field. In these analyses, ozone chemistry appears to be faster than that in the Cariolle v2.1 scheme, which has a photochemical relaxation time of ~100 days at these levels. The improvement in the KNMI SCIAMACHY profile analyses compared to those based on SCIAMACHY total columns may be due to the observations, but these systems also differ in that the profile analyses used of 3-hourly rather than 6-hourly winds, which could have improved transport in the UTLS.

Problems in the DARC analyses are likely due to poor transport. DARC analysis runs that assimilate SBUV instead of MIPAS (not shown here) produce similar structure in the ozone field at the tropopause; hence MIPAS is unlikely to be the cause of the variability in the DARC analyses.

Intercomparison of ozone analyses

A. J. Geer et al.

Title Page

Abstract

Introduction

Conclusions

References

Tables

Figures

◀

▶

◀

▶

Back

Close

Full Screen / Esc

Printer-friendly Version

Interactive Discussion

6 Conclusion

This paper introduces the method, initial results and analysis types involved in the ASSET intercomparison. However, many questions remain that will be answered in more detail in further studies by the partners involved.

5 We have compared 11 different sets of ozone analyses based on 7 different data assimilation systems. Two are NWP systems based on GCMs, and five use CTMs. These systems contain either linearised or detailed ozone chemistry, or in two cases, no chemistry at all. In most analyses, MIPAS ozone data are assimilated. Examples are also shown of SCIAMACHY total column and profile assimilation. The analyses have
10 been interpolated to a common grid and are then compared to ozone profiles from sondes, HALOE, MIPAS, and to total column ozone from TOMS, for the period July to November 2003. Results are presented in percentage terms, relative to a monthly-mean ozone climatology.

15 Through most of the stratosphere (50 hPa to 1 hPa), almost all the systems produce good results. Biases are usually within $\pm 10\%$ compared to sonde, HALOE and MIPAS. Standard deviations of the differences are less than 10%, except in the SH high latitudes ($>60^\circ$ S), where standard deviations increase to 20% at 50 hPa. If the analyses were replaced by zonal mean climatology, standard deviations would be substantially larger, except in the tropical stratosphere where the zonal mean would do just as well
20 as the analyses. The KNMI TEMIS, ECMWF and DARC analyses have some shortcomings in the upper stratosphere (6 to 1 hPa) where biases are larger, in some places reaching 50%. KNMI TEMIS and ECMWF also have standard deviations of $\sim 15\%$ in the polar upper stratosphere. These problems are in general due to poor ozone photochemistry parametrizations, and could be easily remedied by using newer versions;
25 ECMWF ozone analyses may also be affected by known vertical temperature oscillations in these regions (Randel et al., 2004). Also, the top of the MOCAGE-PALM model is at about 5 hPa, and biases slightly larger than 10% are seen at these levels.

Biases and standard deviations are larger in the UTLS, in the troposphere, the meso-

Intercomparison of ozone analyses

A. J. Geer et al.

Title Page

Abstract

Introduction

Conclusions

References

Tables

Figures

◀

▶

◀

▶

Back

Close

Full Screen / Esc

Printer-friendly Version

Interactive Discussion

sphere, and the Antarctic ozone hole region. However, amongst the analyses, some do substantially better than others in each of these regions, indicating that improvements are possible. We summarise these regions:

- At the tropical tropopause, ozone distributions should be relatively uniform, but compared to ozonesondes, many analyses show positive biases (up to 50%) and excessive structure in the ozone fields, resulting in standard deviations up to 35%. The reasons may vary depending upon the system, but the principal causes are likely to be the known deficiencies in tropical wind fields in data assimilation systems, and a degradation in quality of the MIPAS data at these levels. ECMWF do best against ozonesonde observations, by producing a smooth ozone field around the equator at 100 hPa, resulting in standard deviations of 15%, which suggests the wind fields and ozone transport in the system are of good quality. However, ozone amounts are 10% lower than sonde in the ECMWF analyses, perhaps indicative of excessive transport from troposphere to stratosphere. It is important to simulate tropical UTLS ozone well; [Cariolle and Morcrette \(2006\)](#) show that in this region, small changes in the ozone amounts can influence modelled temperatures by several degrees.
- In the SH ozone hole, not all analyses achieve the observed near-complete ozone destruction over the pole during October 2003. The MIMOSA and Juckes analyses show excessively high ozone amounts in the lower stratosphere polar vortex. These systems do not model ozone chemistry and must rely on MIPAS observations, which are noisy and have a small positive bias in these regions. The other analysis systems model heterogeneous ozone depletion in a variety of ways. The simplest approach (included in the Cariolle v1.2 and v2.1 chemistry schemes) is a depletion term which is active in sunlight at temperatures below 195 K. This approach reproduces the near-complete ozone depletion in October in the ECMWF analyses and in the MOCAGE-PALM system. The sophisticated scheme in the Reprobus model, and the PSC parametrization (Chabrilat et al., 2006¹) of the

Intercomparison of ozone analyses

A. J. Geer et al.

Title Page

Abstract

Introduction

Conclusions

References

Tables

Figures

◀

▶

◀

▶

Back

Close

Full Screen / Esc

Printer-friendly Version

Interactive Discussion

**Intercomparison of
ozone analyses**A. J. Geer et al.

Title Page

Abstract

Introduction

Conclusions

References

Tables

Figures

◀

▶

◀

▶

Back

Close

Full Screen / Esc

Printer-friendly Version

Interactive Discussion

BASCOE v3q33 analyses also work well. BASCOE v3d24 analyses uses the PSCBox model (Larsen et al., 2000) but show excessively high ozone amounts of 1 to 2 ppmm in the ozone hole. PSCBox is highly sensitive to temperature and a likely explanation for the problems is biases in the ECMWF temperatures used to drive the CTM (Gobiet et al., 2005). The KNMI TEMIS and DARC analyses used a cold tracer formulation, and did well, but they did not completely deplete ozone in the ozone hole. In the case of the DARC analyses, complete ozone depletion was prevented by erroneous ozone production in the photochemistry scheme.

- In the upper-stratosphere and mesosphere (above 5 hPa), large biases were identified in some analyses, but these were due to the modelled ozone photochemistry. In the case of DARC analyses, the Cariolle scheme was incorrectly implemented. In the case of KNMI TEMIS analyses, use of the LINOZ scheme resulted in excessively low ozone at these levels. Multiplying the O₂ photolysis rates by 1.25 in the BASCOE v3d24 analyses actually reduced biases against independent data by ~10%, suggesting that there are still uncertainties in the chemistry or in the observations at these levels. A feature of the mesosphere above 0.5 hPa is the diurnal cycle in ozone, which is not represented except by models using a detailed chemistry scheme. Only the BASCOE analyses are able to reproduce this. Sassi et al. (2005) show the importance of capturing this diurnal cycle when calculating heating rates in the upper stratosphere and mesosphere. The Jukes analyses, and MIMOSA up to its model top at ~2 hPa, do not model chemistry. However, by assimilating MIPAS data they have biases and standard deviations against independent HALOE data that are typically as low as the BASCOE analyses, throughout the upper stratosphere and mesosphere to the 0.5 hPa level where the diurnal cycle becomes important.
- In the midlatitude UTLS (50 hPa to 400 hPa), where dynamical information is expected to be inferred from ozone distributions, standard deviations against ozonesonde are relatively high. For the best performing analyses in this region

**Intercomparison of
ozone analyses**

A. J. Geer et al.

[Title Page](#)[Abstract](#)[Introduction](#)[Conclusions](#)[References](#)[Tables](#)[Figures](#)[◀](#)[▶](#)[◀](#)[▶](#)[Back](#)[Close](#)[Full Screen / Esc](#)[Printer-friendly Version](#)[Interactive Discussion](#)

(ECMWF in the SH and KNMI TEMIS in the NH) these are 20% to 40%. However, the analyses clearly contain additional information over zonal mean climatology. Further studies are needed in the UTLS.

- 5 – There are wide discrepancies in analysed tropospheric ozone, compared to sonde observations. No analysis system incorporates ozone profile information below 400 hPa, and only the MOCAGE-PALM Reprobus analyses attempt to model tropospheric chemistry realistically. The best performer is the MOCAGE-PALM Reprobus run, with biases less than $\pm 30\%$ through the troposphere. In the KNMI analyses, the linear chemistry schemes have been modified in the troposphere so that they relax to ozone climatology. Particularly in the SCIAMACHY profile run, this is a strategy that appears to minimise bias, as compared to the systems using the unmodified linearised ozone photochemistry schemes, which are designed primarily for the stratosphere. ECMWF and MOCAGE-PALM Cariolle v2.1 analyses have biases within -30% and $+50\%$ between 100 hPa and 700 hPa, though 10 biases in the lower stratosphere are larger, and ECMWF standard deviations are comparatively high. The DARC analyses have larger biases still.

In the stratosphere and mesosphere, MIPAS ozone appears accurate. This is illustrated by the Juckes and MIMOSA systems which rely entirely on MIPAS observations, yet do as well, compared to independent data, as systems with full chemistry. Also, 20 there is a clear improvement in ECMWF analyses when MIPAS is assimilated, compared to analyses made using SBUV and limited GOME observations.

It has been possible to use the analyses as a transfer standard to compare MIPAS observations to independent data from sonde and HALOE. Statistics are calculated from essentially the full set of available MIPAS profiles. We treat MIPAS as a point retrieval, rather than using averaging kernels. Hence, much caution should be exercised before interpreting these results in terms of the calibration of the instrument, but they 25 do reflect the way MIPAS data is used in the assimilation systems:

- In the mid and upper stratosphere and mesosphere (above 30 hPa), MIPAS ozone

is ~5% higher than HALOE.

- In the lower stratosphere (100 hPa to 30 hPa) there are typically positive biases compared to sonde and HALOE of ~10%.
- There is excessive noise in observations around the tropical tropopause, likely due to undetected cloud and the sharp vertical transitions in temperature and ozone.

At the tropopause and below, the choice of vertical interpolation strategy affects the size of the bias calculated, so further conclusions cannot be drawn. However, these difficulties suggest that both these results, and the analyses themselves, could be improved by taking better account of the vertical resolution of observations using averaging kernels, or by direct assimilation of MIPAS radiances.

KNMI have assimilated SCIAMACHY total columns (the TOSOMI product) and limb profiles. The total column analyses do almost as well as the MIPAS-based analyses, compared to independent ozone profile data, and they have generally smaller biases and standard deviations compared to independent TOMS total columns than the MIPAS-based analyses. The assimilation of SCIAMACHY profiles is less successful, and causes a negative bias of up to 20% in the NH between 200 hPa and 30 hPa. It is clear that improvements are needed in the SCIAMACHY limb profile retrievals.

It has been seen that improved ozone analyses can be achieved through better modelled chemistry and transport, and better observations. It is also likely that improvements will come through better modelling of the background errors. In this intercomparison, systems based on very different approaches, i.e. 3D-Var, 4D-Var, Kalman filter or direct inversion, CTM or GCM, show broadly similar agreement with independent data. Due to the nature of the intercomparison, we cannot easily separate the influence of these different techniques from other factors affecting the quality of the analyses. Nevertheless, the different systems vary widely in the amount of computer time used. The isentropic assimilation schemes (Juckes, 2005, and MIMOSA) do well

Intercomparison of ozone analyses

A. J. Geer et al.

Title Page

Abstract

Introduction

Conclusions

References

Tables

Figures

◀

▶

◀

▶

Back

Close

Full Screen / Esc

Printer-friendly Version

Interactive Discussion

**Intercomparison of
ozone analyses**

A. J. Geer et al.

Title Page

Abstract

Introduction

Conclusions

References

Tables

Figures

I◀

▶I

◀

▶

Back

Close

Full Screen / Esc

Printer-friendly Version

Interactive Discussion

against independent observations, and are extremely fast, but do depend on the quality and availability of the MIPAS data. They are not as good in the ozone hole, where there are limitations with the MIPAS observations; the CTMs and GCMs with chemistry do better. The GCM-based analyses require substantially more computer power than the CTM approach, though ozone assimilation is a relatively small additional cost when included in an existing NWP system. It still remains for the proposed benefits of the operational assimilation of ozone in NWP systems (better assimilation of temperature radiances, better heating rates, ozone-radiation feedback, the inference of midlatitude UTLS dynamical information) to be demonstrated with improved forecasts in an operational NWP system.

Acknowledgements. We thank D. Cariolle for many useful comments and discussions. For the use of ozonesonde data, we thank both the individual contributors and the projects and databases from which they were obtained: WOUDC, SHADOZ and NDSC. All MIPAS data is copyright ESA, 2003. This work was funded jointly by the authors' institutions and the Assimilation of Envisat Data project (ASSET, <http://darc.nerc.ac.uk/asset/>), which is a shared-cost project (contract EVK2-CT-2002-00137) co-funded by the Research DG of the European Commission within the RTD activities of the Environment and Sustainable Development sub-programme (5th Framework Programme). The work also benefited from funds from COST action 723.

References

- Andersson, E. and Järvinen, H.: Variational quality control, Q. J. R. Meteorol. Soc., 125, 697–722, 1999. [4501](#)
- Allen, D. R. and Nakamura, N.: Tracer equivalent latitude: A diagnostic tool for isentropic transport studies, J. Atmos. Sci., 60, 287–304, 2003. [4509](#)
- Bhartia, P. K., McPeters, R. D., Mateer, C. L., Flynn, L. E., and Wellemeyer, C.: Algorithm for the estimation of vertical ozone profiles from the backscattered ultraviolet technique, J. Geophys. Res., 101, 18 793–18 806, 1996. [4499](#)
- Bhatt, P. P., Remsberg, E. E., Gordley, L. L., McInerney, J. M., Brackett, V. G., and Russell,

**Intercomparison of
ozone analyses**

A. J. Geer et al.

Title Page

Abstract

Introduction

Conclusions

References

Tables

Figures

◀

▶

◀

▶

Back

Close

Full Screen / Esc

Printer-friendly Version

Interactive Discussion

J. M.: An evaluation of the quality of Halogen Occultation Experiment ozone profiles in the lower stratosphere, *J. Geophys. Res.*, 104, 9261–9275, 1999. [4513](#), [4521](#)

Bregman, A., Krol, M. C., Teyssedre, H., Norton, W. A., Iwi, A., Chipperfield, M., Pitari, G., Sundet, J. K., and Lelieveld, J.: Chemistry-transport model comparison with ozone observations in the midlatitude lowermost stratosphere, *J. Geophys. Res.*, 106, 17 479–17 496, 2001. [4497](#)

Cariolle, D. and Déqué, M.: Southern-Hemisphere Medium-Scale Waves and Total Ozone Disturbances in a Spectral General Circulation Model, *J. Geophys. Res.*, 91, 10 825–10 846, 1986. [4500](#), [4501](#), [4502](#), [4503](#), [4506](#), [4527](#), [4531](#)

Cariolle, D. and Morcrette, J.-J.: A linearized approach to the radiative budget of the stratosphere: influence of the ozone distribution, *Geophys. Res. Lett.*, 33, L05806, doi:10.1029/2005GL025597, 2006. [4498](#), [4534](#)

Carslaw, K. S., Luo, B., and Peter, T.: An analytic expression for the composition of aqueous $\text{HNO}_3\text{--H}_2\text{SO}_4$ stratospheric aerosols including gas phase removal of HNO_3 , *Geophys. Res. Lett.*, 22, 1877–1880, 1995. [4506](#), [4548](#)

Cathala, M.-L., Pailleux, J., and Peuch, V.-H.: Improving global simulations over the upper troposphere-lower stratosphere with sequential assimilation of MOZAIC data, *Tellus*, 55B, 1–10, 2003. [4498](#), [4506](#)

Chipperfield, M. P., Khattatov, B. V., and Lary, D. J.: Sequential assimilation of stratospheric chemical observations in a three-dimensional model, *J. Geophys. Res.*, 107, 4585, doi:10.1029/2002JD002110, 2002. [4498](#)

Courtier, P., Freyrier, C., Geleyn, J.-F., Rabier, F., and Rochas, M.: The ARPEGE project at Météo-France, ECMWF seminar proceedings, Reading, 9–13 Sept. 1991, vol. II, pp. 193–231, 1991. [4506](#)

Davies, T., Cullen, M. J. P., Malcolm, A. J., Mawson, M. H., Staniforth, A., White, A. A., and Wood, N.: A new dynamical core for the Met Office's global and regional modelling of the atmosphere, *Q. J. R. Meteorol. Soc.*, 131, 1759–1782, 2005. [4502](#)

Dethof, A.: Assimilation of ozone retrievals from the MIPAS instrument on board ENVISAT, ECMWF Technical Memoranda, 428, <http://www.ecmwf.int/publications/>, 2003a. [4499](#), [4501](#), [4511](#), [4523](#), [4525](#)

Dethof, A.: Monitoring of retrievals from the MIPAS and SCIAMACHY instruments on board ENVISAT, Contract Report to the European Space Agency, European Centre for Medium-Range Weather Forecasts, available from <http://www.ecmwf.int>, 2003b. [4511](#), [4523](#), [4524](#)

**Intercomparison of
ozone analyses**

A. J. Geer et al.

Title Page

Abstract

Introduction

Conclusions

References

Tables

Figures

◀

▶

◀

▶

Back

Close

Full Screen / Esc

Printer-friendly Version

Interactive Discussion

- Dethof, A.: Monitoring and assimilation of MIPAS, SCIAMACHY and GOMOS retrievals at ECMWF, Contract Report to the European Space Agency, European Centre for Medium-Range Weather Forecasts, available from <http://www.ecmwf.int>, 2004. 4511, 4519, 4523
- 5 Dethof, A. and Hólm, E. V.: Ozone assimilation in the ERA-40 reanalysis project, Q. J. R. Meteorol. Soc., 130, 2851–2872, 2004. 4499, 4501, 4528
- Dufour, A., Amodei, M., Ancellet, G., and Peuch, V.-H.: Observed and modelled ‘chemical weather’ during ESCOMPTE, Atmos. Res., 74, 161–189, 2004. 4506
- El Amraoui, L., Ricaud, P., Urban, J., Theodore, B., Hauchecorne, A., Lautie, N., De La Noe, J., Guirlet, M., Le Flochmoen, E., Murtagh, D., Dupuy, E., Frisk, U., and d’Andon, O. F.: Assimilation of Odin/SMR O₃ and N₂O measurements in a three-dimensional chemistry transport model, J. Geophys. Res., 109, D22304, doi:10.1029/2004JD004796, 2004. 4498
- 10 Elbern, H. and Schmidt, H.: Ozone episode analysis by four-dimensional variational chemistry data assimilation, J. Geophys. Res., 106, 3569–3590, 2001. 4498
- Eskes, H. J., Van Velthoven, P. F. J., Valks, P. J. M., and Kelder, H. M.: Assimilation of GOME total-ozone satellite observations in a three-dimensional tracer-transport model, Q. J. R. Meteorol. Soc., 129, 1663–1681, 2003. 4498, 4502, 4503, 4529
- 15 Eskes, H. J., Segers, A. J., and Van Velthoven, P. F. J.: Ozone forecasts of the Stratospheric Polar Vortex Splitting Event in September 2002, J. Atmos. Sci., 62, 812–821, 2005a. 4498
- Eskes, H. J., van der A, R. J., Brinksma E. J., Veefkind, J. P., de Haan, J. F., and Valks, P. J. M.: Retrieval and validation of ozone columns derived from measurements of SCIAMACHY on Envisat, Atmos. Chem. Phys. Discuss., 5, 4429–4475, 2005b. 4503
- 20 Errera, Q. and Fonteyn, D.: Four-dimensional variational chemical assimilation of CRISTA stratospheric measurements, J. Geophys. Res., 106, 12 253–12 265, 2001. 4498, 4504
- European Space Agency: MIPAS Product Handbook, issue 1.2, available from <http://envisat.esa.int/dataproducts>, 2004. 4511
- 25 Fierli, F., Hauchecorne, A., Bekki, S., Theodore, B., and Fanton D’Andon, O.: Data assimilation of stratospheric ozone using a high-resolution transport model, Geophys. Res. Lett., 29, doi:10.1029/2001GL014272, 2002. 4498, 4507
- Fischer, H. and Oelhaf, H.: Remote sensing of vertical profiles of atmospheric trace constituents with MIPAS limb-emission spectrometers, Appl. Opt., 35, 2787–2796, 1996. 4511
- 30 Fischer, H. and Oelhaf, H.: Summary of the MIPAS validation results, Proceedings of the Second Workshop on the Atmospheric Chemistry Validation of Envisat (ACVE-2), 3–7th May 2004, ESA-ESRIN, Frascati, Italy, ESA SP-562, <http://envisat.esa.int/workshops/acve2/>

contents.html, 2004. [4511](#), [4523](#)

Fisher, M.: Background error covariance modelling, Proceedings of the ECMWF Seminar on recent developments in data assimilation from atmosphere and ocean, 8–12 September 2003, ECMWF, Reading, UK, pp. 45–64, 2003. [4502](#)

5 Fisher, M. and Andersson, E.: Developments in 4D-Var and Kalman Filtering, ECMWF Technical Memoranda, 347, 2001. [4506](#)

Fisher, M. and Lary, D. J.: Lagrangian 4-dimensional variational data assimilation of chemical-species, Q. J. R. Meteorol. Soc., 121, 1681–1704, 1995. [4498](#)

10 Fortuin, J. P. F. and Kelder, H.: An ozone climatology based on ozonesonde and satellite measurements, J. Geophys. Res., 103, 31 709–31 734, 1998. [4508](#), [4520](#)

Fortuin, J. P. F. and Langematz, U.: An update on the global ozone climatology and on concurrent ozone and temperature trends, SPIE Proceedings Series, Vol. 2311, Atmos. Sens. Modeling, pp. 207–216, 1995. [4502](#)

15 Gauthier, P., Chouinard, C., and Brasnett, B.: Quality control: Methodology and applications, Data Assimilation for the Earth System, edited by: Swinbank, R., Shutyaev, V., and Lahoz, W. A.: Kluwer Academic Publications, Dordrecht, The Netherlands, pp. 177–187, 2003. [4504](#)

Geer, A. J., Peubey, C., Bannister, R. N., Brugge, R., Jackson, D. R., Lahoz, W. A., Migliorini, S., O'Neill, A., and Swinbank, R.: Assimilation of stratospheric ozone from MIPAS into a global general circulation model: the September 2002 vortex split, Q. J. R. Meteorol. Soc., 20 132, 231–257, 2006. [4498](#), [4499](#), [4502](#), [4503](#), [4511](#), [4523](#), [4525](#), [4526](#), [4529](#)

Gobiet, A., Foelsche, U., Steiner, A. K., Borsche, M., Kirchengast, G., and Wickert, J.: Climatological validation of stratospheric temperatures in ECMWF operational analyses with CHAMP radio occultation data, Geophys. Res. Lett., 32, L12806, doi:10.1029/2005GL022617, 2005. [4529](#), [4535](#)

25 Hervig, M. and McHugh, M.: Cirrus detection using HALOE measurements, Geophys. Res. Lett., 26, 719–722, 1999. [4513](#)

Hoepfner, M., Larsen, N., Spang, R., Luo, B. P., Ma, J., Svendsen, S. H., Eckermann, S. D., Knudsen, B., Massoli, P., Cairo, F., Stiller, G., von Clarmann, T., and Fischer, H.: MIPAS detects Antarctic stratospheric belt of NAT PSCs caused by mountain waves, Atmos. Chem. 30 Phys., 6, 1221–1230, 2006. [4529](#)

Hudson, R. D., Frolov, A. D., Andrade, M. F., and Follette, M. B.: The total ozone field separated into meteorological regimes. Part I: defining the regimes, J. Atmos. Sci., 60, 1669–1677, 2003. [4520](#)

**Intercomparison of
ozone analyses**

A. J. Geer et al.

Title Page

Abstract

Introduction

Conclusions

References

Tables

Figures

◀

▶

◀

▶

Back

Close

Full Screen / Esc

Printer-friendly Version

Interactive Discussion

**Intercomparison of
ozone analyses**A. J. Geer et al.

Title Page

Abstract

Introduction

Conclusions

References

Tables

Figures

◀

▶

◀

▶

Back

Close

Full Screen / Esc

Printer-friendly Version

Interactive Discussion

- Jackson, D. R.: Improvements in data assimilation at the Met Office, Met Office Forecasting Research Technical Report, 454, 2004. [4502](#)
- Jackson, D. R. and Saunders, R.: Ozone Data Assimilation: Preliminary System, Met Office Forecasting Research Technical Report, 394, 2002. [4502](#)
- 5 Josse, B., Simon, P., and Peuch V.-H.: Radon global simulations with the multiscale chemistry and transport model MOCAGE, Tellus, 56B, 339–356, 2004. [4506](#)
- Juckes, M. N.: The direct inversion method for data assimilation using isentropic tracer advection, Atmos. Chem. Phys. Discuss., 5, 8879–8923, 2005. [4507](#), [4518](#), [4537](#), [4548](#)
- 10 Kalnay, E.: Atmospheric modeling, data assimilation and predictability, Cambridge University Press, UK, 2003. [4497](#), [4503](#), [4505](#), [4507](#), [4509](#)
- Khattatov, B. V., Lamarque, J. F., Lyjak, L. V., Ménard, R., Levelt, P., Tie, X. X., Brasseur, G. P. and Gille, J. C.: Assimilation of satellite observations of long-lived chemical species in global chemistry transport models, J. Geophys. Res., 105, 29 135–29 144, 2000. [4498](#)
- 15 Komhyr, W. D., Barnes, R. A., Brothers, G. B., Lathrop, J. A., and Opperman, D. P.: Electrochemical Concentration Cell Ozonesonde Performance Evaluation During STOIC 1989, J. Geophys. Res., 100, 9231–9244, 1995. [4512](#)
- Lagarde, T., Piacentini, A., and Thual, O.: A New Representation of Data Assimilation Methods: the PALM Flow Charting Approach, Q. J. R. Meteorol. Soc., 127, 189–207, 2001. [4506](#)
- Lahoz, W. A., Geer, A. J., and O'Neill, A.: Dynamical evolution of the 2003 southern hemisphere stratospheric winter using Envisat trace-gas observations, Q. J. R. Meteorol. Soc., accepted, 2006. [4500](#), [4509](#), [4512](#), [4520](#), [4528](#)
- 20 Larsen, N.: Polar Stratospheric Clouds. Microphysical and optical models, Scientific report 00-06, Danish Meteorological Institute, available from <http://www.dmi.dk/>, 2000. [4504](#), [4529](#), [4535](#)
- 25 Larsen, N., Svendsen, S. H., Knudsen, B. M., Voigt, C., Weisser, C., Kohlmann, A., Schreiner, J., Mauersberger, K., Deshler, T., Kröger, C., Rosen, J. M., Kjome, N. T., Adriani, A., Cairo, F., Di Donfrancesco, G., Ovarlez, J., Ovarlez, H., Dörnbrack, A., and Birner, T.: Microphysical mesoscale simulations of polar stratospheric cloud formation constrained by in situ measurements of chemical and optical cloud properties, J. Geophys. Res., 107, 8301, doi:10.1029/2001JD000999, 2002. [4529](#)
- 30 Larsen, N., Knudsen, B. M., Svendsen, S. H., Deshler, T., Rosen, J. M., Kivi, R., Weisser, C., Schreiner, J., Mauerberger, K., Cairo, F., Ovarlez, J., Oelhaf, H., and Spang, R.: Formation of solid particles in synoptic-scale Arctic PSC's in early winter 2002/2003, Atmos. Chem.

**Intercomparison of
ozone analyses**

A. J. Geer et al.

Title Page

Abstract

Introduction

Conclusions

References

Tables

Figures

◀

▶

◀

▶

Back

Close

Full Screen / Esc

Printer-friendly Version

Interactive Discussion

Phys., 4, 2001–2013, 2004. [4529](#)

Lefèvre, F., Brasseur, G. P., Folkins, I., Smith, A. K., and Simon, P.: Chemistry of the 1991–1992 stratospheric winter: three-dimensional model simulations, *J. Geophys. Res.*, 99(D4), 8183–8195, 1994. [4506](#), [4548](#)

5 Lefèvre, F., Figarol, F., Carslaw, K. S., and Peter, T.: The 1997 Arctic ozone depletion quantified from three-dimensional model simulations, *Geophys. Res. Lett.*, 25, 2425–2428, 1998. [4506](#)

Li, D. and Shine K. P.: A 4-dimensional ozone climatology for UGAMP models, *UGAMP Int. Rep.*, 35, April 1995. [4502](#)

10 Logan, J. A.: An analysis of ozonesonde data for the troposphere: Recommendations for testing 3-D models and development of a gridded climatology for tropospheric ozone, *J. Geophys. Res.*, 104, 16 115–16 149, 1999. [4508](#), [4525](#), [4526](#), [4571](#)

Lorenc, A. C., Ballard, S. P., Bell, R. S., Ingleby, N. B., Andrews, P. L. F., Barker, D. M., Bray, J. R., Clayton, A. M., Dalby, T. D., Li, D., Payne, T. J., and Saunders, F. W.: The Met. Office global three-dimensional variational data assimilation scheme, *Q. J. R. Meteorol. Soc.*, 126, 2991–3012, 2000. [4502](#)

15 McCormack, J. P., Eckermann, S. D., Coy, L., Allen, D. R., Kim, Y.-J., Hogan, T., Lawrence, B., Stephens, A., Browell, E. V., Burris, J., McGee, T., and Trepte, C. R.: NOGAPS-ALPHA model simulations of stratospheric ozone during the SOLVE2 campaign, *Atmos. Chem. Phys.*, 4, 2401–2423, 2004. [4500](#), [4527](#)

20 McLinden, C. A., Olsen, S. C., Hannegan, B., Wild, O., Prather, M. J., and Sundet, J.: Stratospheric ozone in 3-D models: A simple chemistry and the cross-tropopause flux, *J. Geophys. Res.*, 105, 14 653–14 665, 2000. [4500](#), [4503](#), [4527](#)

McPeters, R. D., Bhartia, P. K., Krueger, A. J., Herman, J. R., Wellemeyer, C. G., Seftor, C. J., Jaross, G., Torres, O., Moy, L., Labow, G., Byerly, W., Taylor, S. L., Swissler, T., and Cebula, R. P.: Earth Probe Total Ozone Mapping Spectrometer (TOMS) Data Products User's Guide, NASA Technical Publication 1998-206895, NASA Goddard Space Flight Center, Greenbelt, Maryland 20771, 1998. [4514](#)

25 Massart, S., Cariolle, D., and Peuch, V.-H.: Towards an improvement of the atmospheric ozone distribution and variability by assimilation of satellite data, *C. R. Geosciences*, 15, 1305–1310, 2005. [4499](#), [4505](#)

30 Migliorini, S., Piccolo, C., and Rodgers, C. D.: Intercomparison of direct and indirect measurements: Michelson Interferometer for Passive Atmospheric Sounding (MIPAS) versus sonde ozone profiles, *J. Geophys. Res.*, 109, D19316, doi:10.1029/2004JD004988, 2004. [4511](#),

4522, 4523

Morcrette, J. J.: Ozone-radiation interactions in the ECMWF forecast system, ECMWF Technical Memoranda, 375, 2003. [4498](#)

Peuch, A., Thépaut, J.-N., and Pailleux, J.: Dynamical impact of total-ozone observations in a four-dimensional variational assimilation, Q. J. R. Meteorol. Soc., 126, 1641–1659, 2000. [4498](#), [4520](#)

Plumb, R. A.: Stratospheric transport, J. Meteorol. Soc. Jpn., 80, 793–809, 2002. [4531](#)

Rabier, F., Jarvinen, H., Klinker, E., Mahfouf, J. F., and Simmons, A.: The ECMWF operational implementation of four-dimensional variational assimilation. I: Experimental results with simplified physics, Q. J. R. Meteorol. Soc., 126, 1148–1170, 2000. [4502](#)

Randel, W., Udelhofen, P., Fleming, E., Geller, M., Gelman, M., Hamilton, K., Karoly, D., Orland, D., Pawson, S., Swinbank, R., Wu, F., Baldwin, M., Chanin, M. L., Keckhut, P., Labitzke, K., Remsberg, E., Simmons, A., and Wu, D.: The SPARC intercomparison of middle-atmosphere climatologies, J. Climate, 17, 986–1003, 2004. [4521](#), [4533](#)

Randel, W. J., Wu, F., Russell, J. M., Roche, A., and Waters, J. W.: Seasonal cycles and QBO variations in stratospheric CH₄ and H₂O observed in UARS HALOE data, J. Atmos. Sci., 55, 163–185, 1998. [4509](#)

Riishøjgaard, L. P.: On four-dimensional variational assimilation of ozone data in weather-prediction models, Q. J. R. Meteorol. Soc., 122, 1545–1571, 1996. [4498](#), [4502](#), [4520](#)

Rodgers, C. D.: Inverse Methods for Atmospheric Sounding: Theory and Practice, World Scientific Publishing, Singapore, 2000. [4522](#)

Roelofs, G. J., Kentarchos, A. S., Trickl, T., Stohl, A., Collins, W. J., Crowther, R. A., Hauglustaine, D., Klonecki, A., Law, K. S., Lawrence, M. G., von Kuhlmann, R., and van Weele, M.: Intercomparison of tropospheric ozone models: Ozone transport in a complex tropopause folding event, J. Geophys. Res., 108, 8529, doi:10.1029/2003JD003462, 2003. [4497](#)

Russell, J. M., Gordley, L. L., Park, J. H., Drayson, S. R., Hesketh, W. D., Cicerone, R. J., Tuck, A. F., Frederick, J. E., Harries, J. E., and Crutzen, P. J.: The Halogen Occultation Experiment, J. Geophys. Res., 98, 10777–10797, 1993. [4513](#)

Sassi, F., Boville, B. A., Kinnison, D., and Garcia, R. R.: The effects of interactive ozone chemistry on simulations of the middle atmosphere, Geophys. Res. Lett., 32, L07811, doi:10.1029/2004GL022131, 2005. [4498](#), [4535](#)

Scheele, M. P., Siegmund, P. C., and van Velthoven, P. F. J.: Stratospheric age of air computed with trajectories based on various 3-D-Var and 4-D-Var data sets, Atmos. Chem. Phys., 5,

ACPD

6, 4495–4577, 2006

Intercomparison of ozone analyses

A. J. Geer et al.

Title Page

Abstract

Introduction

Conclusions

References

Tables

Figures

◀

▶

◀

▶

Back

Close

Full Screen / Esc

Printer-friendly Version

Interactive Discussion

EGU

1–7, 2005. [4531](#)

Schoeberl, M. R., Douglass, A. R., Zhu, Z. X. and Pawson, S.: A comparison of the lower stratospheric age spectra derived from a general circulation model and two data assimilation systems, *J. Geophys. Res.*, 108, 4113, doi:10.1029/2002JD002652, 2003. [4531](#)

5 Segers, A. J., Eskes, H. J., Van Der A, R. J., Van Oss, R. F., and Van Velthoven, P. F. J.: Assimilation of GOME ozone profiles and a global chemistry transport model using a Kalman filter with anisotropic covariance, *Q. J. R. Meteorol. Soc.*, 131, 477–502, 2005a. [4499](#), [4504](#)

Segers, A. J., Von Savigny, C., Brinksma, E. J., and Piters, A. J. M.: Validation of IFE-1.6 SCIAMACHY limb ozone profiles, *Atmos. Chem. Phys.*, 5, 3045–3052, 2005b. [4503](#)

10 Spiegel, M. R. and Stephens, L. J.: *Schaum's Outline of Theory and Problems of Statistics*, 3rd Ed., McGraw-Hill, New York, 538pp., 1999. [4525](#)

Štajner, I., Riishøjgaard, L. P., and Rood, R. B.: The GEOS ozone data assimilation system: Specification of error statistics, *Q. J. R. Meteorol. Soc.*, 127, 1069–1094, 2001. [4498](#)

Štajner, I., Winslow, N., Rood, R. B., and Pawson, S.: Monitoring of observation errors in the assimilation of satellite ozone data, *J. Geophys. Res.*, 109, D06309, doi:10.1029/2003JD004118, 2004. [4510](#)

Stohl, A., Cooper, O. R., and James, P.: A cautionary note on the use of meteorological analysis fields for quantifying atmospheric mixing, *J. Atmos. Sci.*, 61, 1446–1453, 2004. [4532](#)

20 Struthers, H., Brugge, R., Lahoz, W. A., O'Neill, A., and Swinbank, R.: Assimilation of ozone profiles and total column measurements into a global general circulation model, *J. Geophys. Res.*, 107, 4438, doi:10.1029/2001JD000957, 2002. [4499](#), [4518](#)

Talagrand, O.: A posteriori validation of assimilation algorithms, *Data Assimilation for the Earth System*, edited by: Swinbank, R., Shutyaev, V., and Lahoz, W. A., Kluwer Academic Publications, Dordrecht, The Netherlands, 85–95, 2003. [4510](#)

25 Tan, W. W., Geller, M. A., Pawson, S., and da Silva, A.: A case study of excessive subtropical transport in the stratosphere of a data assimilation system, *J. Geophys. Res.*, 109, D11102, doi:10.1029/2003JD004057, 2004. [4531](#)

Thompson, A. M., Witte, J. C., McPeters, R. D., Oltmans, S. J., Schmidlin, F. J., Logan, J. A., Fujiwara, M., Kirchhoff, V. W. J. H., Posny, F., Coetzee, G. J. R., Hoegger, B., Kawakami, S., Ogawa, T., Johnson, B. J., Vomel, H., and Labow, G.: Southern Hemisphere Additional Ozonesondes (SHADOZ) 1998–2000 tropical ozone climatology – 1. Comparison with Total Ozone Mapping Spectrometer (TOMS) and ground-based measurements, *J. Geophys. Res.*, 108, 8238, doi:10.1029/2001JD000967, 2003a. [4512](#), [4531](#)

ACPD

6, 4495–4577, 2006

Intercomparison of ozone analyses

A. J. Geer et al.

Title Page

Abstract

Introduction

Conclusions

References

Tables

Figures

◀

▶

◀

▶

Back

Close

Full Screen / Esc

Printer-friendly Version

Interactive Discussion

EGU

- Thompson, A. M., Witte, J. C., Oltmans, S. J., Schmidlin, F. J., Logan, J. A., Fujiwara, M., Kirchhoff, V. W. J. H., Posny, F., Coetzee, G. J. R., Hoegger, B., Kawakami, S. J., Ogawa, T., Fortuin, J. P. F., and Kelder, H. M.: Southern Hemisphere Additional Ozonesondes (SHADOZ) 1998–2000 tropical ozone climatology – 2. Tropospheric variability and the zonal wave-one, *J. Geophys. Res.*, 108, 8241, doi:10.1029/2002JD002241, 2003b. [4512](#), [4526](#)
- Wargan, K., Štajner, I., Pawson, S., and Rood, R. B.: Monitoring and Assimilation of Ozone Data from the Michelson Interferometer for Passive Atmospheric Sounding, *Q. J. R. Meteorol. Soc.*, 131, 2713–2734, 2005. [4499](#), [4511](#), [4523](#)
- Weaver, A. and Courtier, P.: Correlation modelling on the sphere using a generalized diffusion equation, *Q. J. R. Meteorol. Soc.*, 127, 1815–1846, 2001. [4507](#)
- World Meteorological Organisation: Scientific assessment of ozone depletion: 2002, Global Ozone Research and Monitoring Project-Report No. 47, 498 pp., Geneva, 2003. [4497](#), [4501](#)
- Žagar, N.: Assimilation of equatorial waves by line-of-sight wind observations, *J. Atmos. Sci.*, 61, 1877–1893, 2004. [4531](#)

**Intercomparison of
ozone analyses**

A. J. Geer et al.

Title Page

Abstract

Introduction

Conclusions

References

Tables

Figures

I◀

▶I

◀

▶

Back

Close

Full Screen / Esc

Printer-friendly Version

Interactive Discussion

Table 1. Principal features of the analysis systems and climatologies.

Name	Type	Winds	Scheme	Ozone observations	Ozone photo-chemistry	Heterogeneous ozone chemistry
ECMWF operational	NWP	GCM	4D-Var	SBUV, GOME total columns, MIPAS from 7/10/2003	Cariolle v1.2	$T < 195$ K term
ECMWF MIPAS	NWP	GCM	4D-Var	SBUV, GOME total columns, MIPAS throughout	Cariolle v1.2	$T < 195$ K term
DARC / Met Office	NWP	GCM	3D-Var	MIPAS	Cariolle v1.0	Cold tracer
KNMI TEMIS	CTM	ECMWF	sub-optimal KF	SCIAMACHY TOSOMI total columns	LINOZ	Cold tracer
KNMI SCIAMACHY profiles	CTM	ECMWF	sub-optimal KF	SCIAMACHY profiles	Cariolle v1.0	Cold tracer
BASCOE v3d24	CTM	ECMWF	4D-Var	MIPAS	57 species	PSCBox
BASCOE v3q33	CTM	ECMWF	4D-Var	MIPAS	57 species	PSC parametrization

Intercomparison of ozone analyses

A. J. Geer et al.

Title Page

Abstract

Introduction

Conclusions

References

Tables

Figures

◀

▶

◀

▶

Back

Close

Full Screen / Esc

Printer-friendly Version

Interactive Discussion

Intercomparison of
ozone analyses

A. J. Geer et al.

Title Page

Abstract

Introduction

Conclusions

References

Tables

Figures

I◀

▶I

◀

▶

Back

Close

Full Screen / Esc

Printer-friendly Version

Interactive Discussion

Table 1. Continued.

Name	Type	Winds	Scheme	Ozone observations	Ozone photo-chemistry	Heterogeneous ozone chemistry
MOCAGE-PALM/Cariolle	CTM	Arpege	3D-FGAT	MIPAS	Cariolle v2.1	$T < 195$ K term
MOCAGE-PALM/Reprobus	CTM	Arpege	3D-FGAT	MIPAS	REPROBUS (Lefèvre et al., 1994)	Carslaw et al. (1995)
MIMOSA	CTM	ECMWF	sub-optimal KF	MIPAS	None	None
Juckes (2005)	CTM	ECMWF	Direct inversion	MIPAS	None	None
Logan/ Fortuin/ Kelder	climatology					
MLS/HALOE mapped by PV	climatology					

Intercomparison of
ozone analyses

A. J. Geer et al.

Title Page

Abstract

Introduction

Conclusions

References

Tables

Figures

◀

▶

◀

▶

Back

Close

Full Screen / Esc

Printer-friendly Version

Interactive Discussion

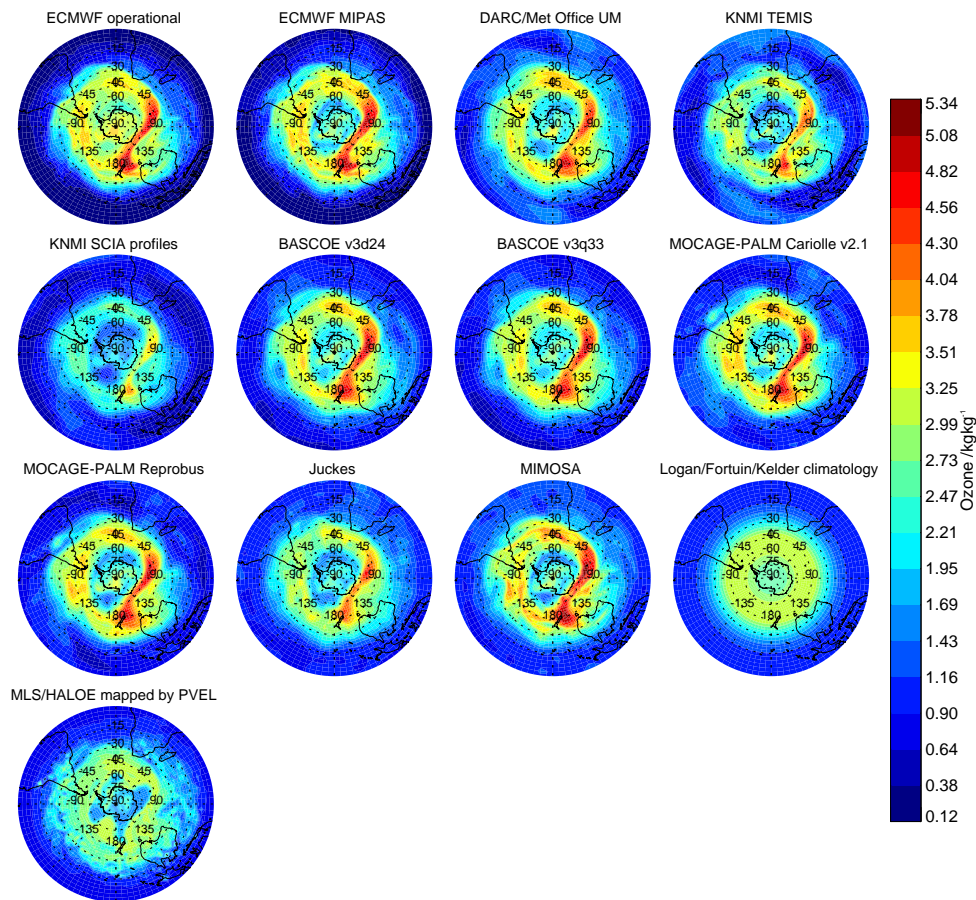


Fig. 1. Ozone (ppmm) at 68 hPa in the southern hemisphere on 31 August 2003, shown on a polar stereographic projection bounded by the equator.

Intercomparison of
ozone analyses

A. J. Geer et al.

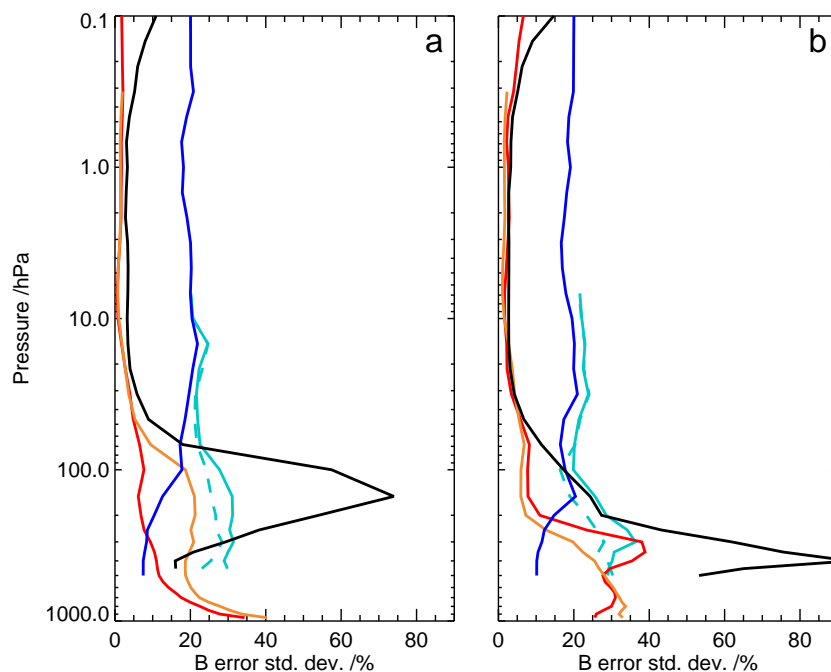


Fig. 2. Standard deviation of ozone background error, given as a percentage relative to climatological ozone, averaged for the period 7 October 2003 to 31 October 2003 in the regions **(a)** 30° S to 30° N and **(b)** 60° S to 90° S, for the analysis systems of ECMWF, DARC, BASCOE and MOCAGE-PALM (see key in Fig. 3). MIPAS error standard deviations, averaged for the same region and time period, are shown by the black line.

[Title Page](#)[Abstract](#)[Introduction](#)[Conclusions](#)[References](#)[Tables](#)[Figures](#)[◀](#)[▶](#)[◀](#)[▶](#)[Back](#)[Close](#)[Full Screen / Esc](#)[Printer-friendly Version](#)[Interactive Discussion](#)

EGU

**Intercomparison of
ozone analyses**

A. J. Geer et al.

-----	ECMWF operational
————	ECMWF MIPAS
————	DARC/Met Office UM
-----	KNMI SCIA profiles
————	KNMI TEMIS
-----	BASCOE v3d24
————	BASCOE v3q33
————	MOCAGE-PALM Cariolle v2.1
-----	MOCAGE-PALM Reprobus
————	Juckes
————	MIMOSA
————	Logan/Fortuin/Kelder climatology

Fig. 3. Key to the analyses. Typically only a subset of these are shown in any one figure.

[Title Page](#)[Abstract](#)[Introduction](#)[Conclusions](#)[References](#)[Tables](#)[Figures](#)[I◀](#)[▶I](#)[◀](#)[▶](#)[Back](#)[Close](#)[Full Screen / Esc](#)[Printer-friendly Version](#)[Interactive Discussion](#)

Intercomparison of
ozone analyses

A. J. Geer et al.

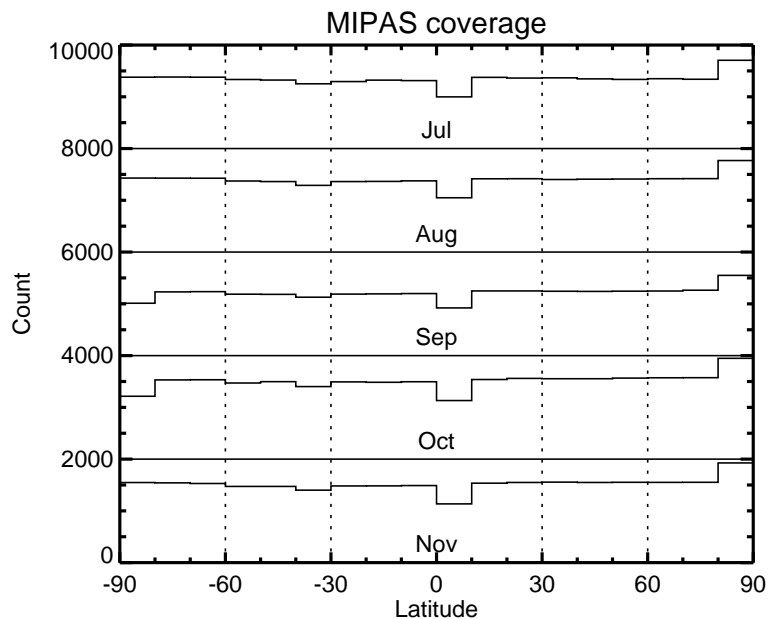


Fig. 4. Number of MIPAS profiles used for validation, by latitude (in 10° bins) and by month, for July to November 2003. Histograms for different months have been staggered by an interval of 2000 counts.

[Title Page](#)[Abstract](#)[Introduction](#)[Conclusions](#)[References](#)[Tables](#)[Figures](#)[◀](#)[▶](#)[◀](#)[▶](#)[Back](#)[Close](#)[Full Screen / Esc](#)[Printer-friendly Version](#)[Interactive Discussion](#)

EGU

Intercomparison of
ozone analyses

A. J. Geer et al.

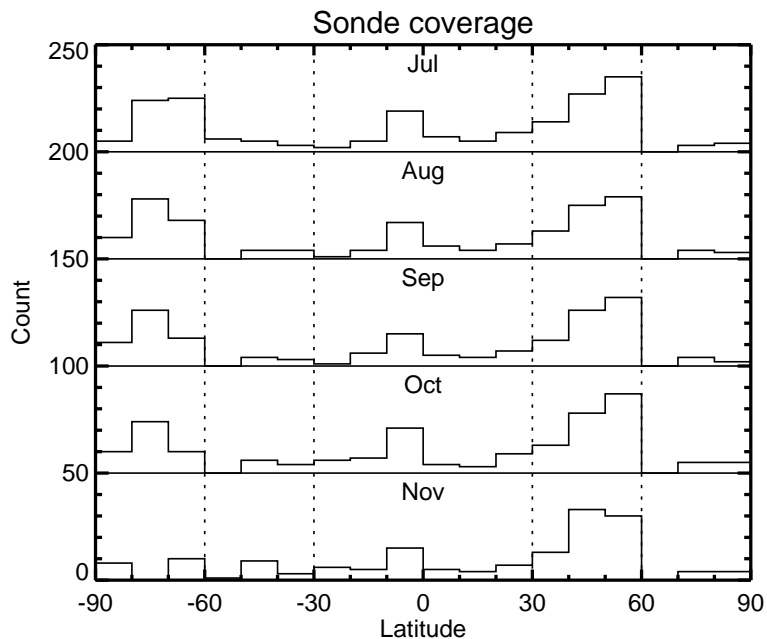


Fig. 5. Number of ozonesonde profiles used for validation, by latitude (in 10° bins) and by month, for July to November 2003. Histograms for different months have been staggered by an interval of 50 counts.

[Title Page](#)[Abstract](#)[Introduction](#)[Conclusions](#)[References](#)[Tables](#)[Figures](#)[◀](#)[▶](#)[◀](#)[▶](#)[Back](#)[Close](#)[Full Screen / Esc](#)[Printer-friendly Version](#)[Interactive Discussion](#)

EGU

Intercomparison of
ozone analyses

A. J. Geer et al.

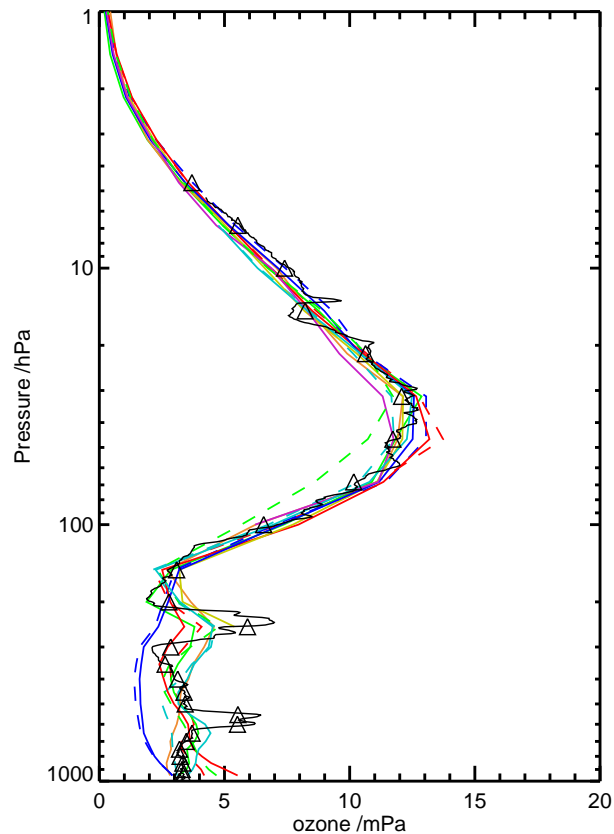


Fig. 6. Example of comparison between sonde ozone at full resolution (black line), layer-averaged (black triangles) and the analyses (key in Fig. 3) at 11:36 UTC on 24 September 2003 at Legionowo (21.0° E, 52.4° N).

[Title Page](#)[Abstract](#)[Introduction](#)[Conclusions](#)[References](#)[Tables](#)[Figures](#)[◀](#)[▶](#)[◀](#)[▶](#)[Back](#)[Close](#)[Full Screen / Esc](#)[Printer-friendly Version](#)[Interactive Discussion](#)

Intercomparison of
ozone analyses

A. J. Geer et al.

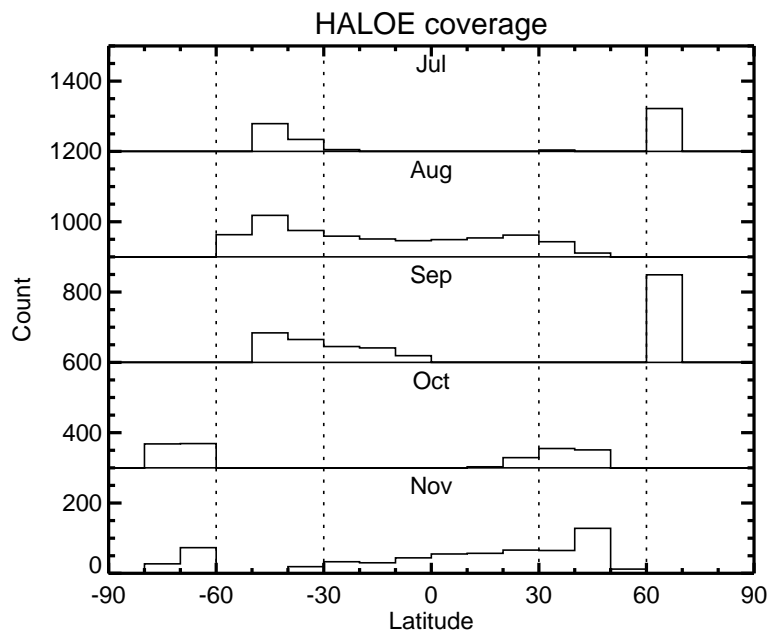


Fig. 7. Number of HALOE profiles used for validation, by latitude (in 10° bins) and by month, for July to November 2003. Histograms for different months have been staggered by an interval of 300 counts.

[Title Page](#)[Abstract](#)[Introduction](#)[Conclusions](#)[References](#)[Tables](#)[Figures](#)[◀](#)[▶](#)[◀](#)[▶](#)[Back](#)[Close](#)[Full Screen / Esc](#)[Printer-friendly Version](#)[Interactive Discussion](#)

EGU

Intercomparison of
ozone analyses

A. J. Geer et al.

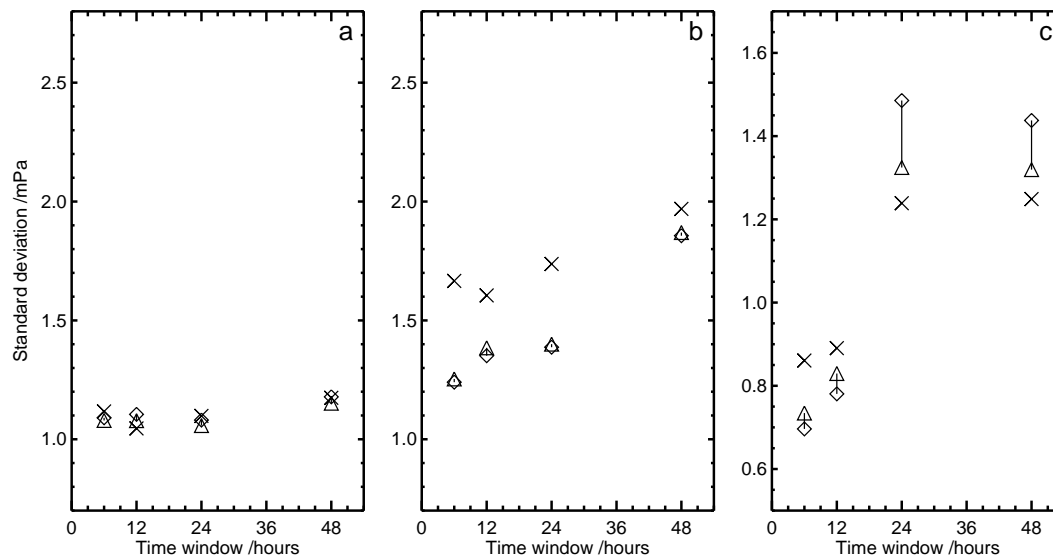


Fig. 8. Effect of varying horizontal and temporal resolution in comparisons between analysed and sonde ozone. The figure shows standard deviation of (analysis – sonde) for 8 October 2003 to 28 November 2003 for: **(a)** 30° S to 30° N at 32 hPa **(b)** 60° S to 90° S at 32 hPa and **(c)** 30° N to 60° N at 200 hPa. Crosses represent DARC analyses at 3.75° by 2.5° resolution. Diamonds represent ECMWF operational analyses reduced to Gaussian N80 resolution (approximately 1.125° by 1.125°). These are joined by a line to triangles representing ECMWF operational analyses reduced to 3.75° by 2.5° resolution.

Title Page

Abstract

Introduction

Conclusions

References

Tables

Figures

◀

▶

◀

▶

Back

Close

Full Screen / Esc

Printer-friendly Version

Interactive Discussion

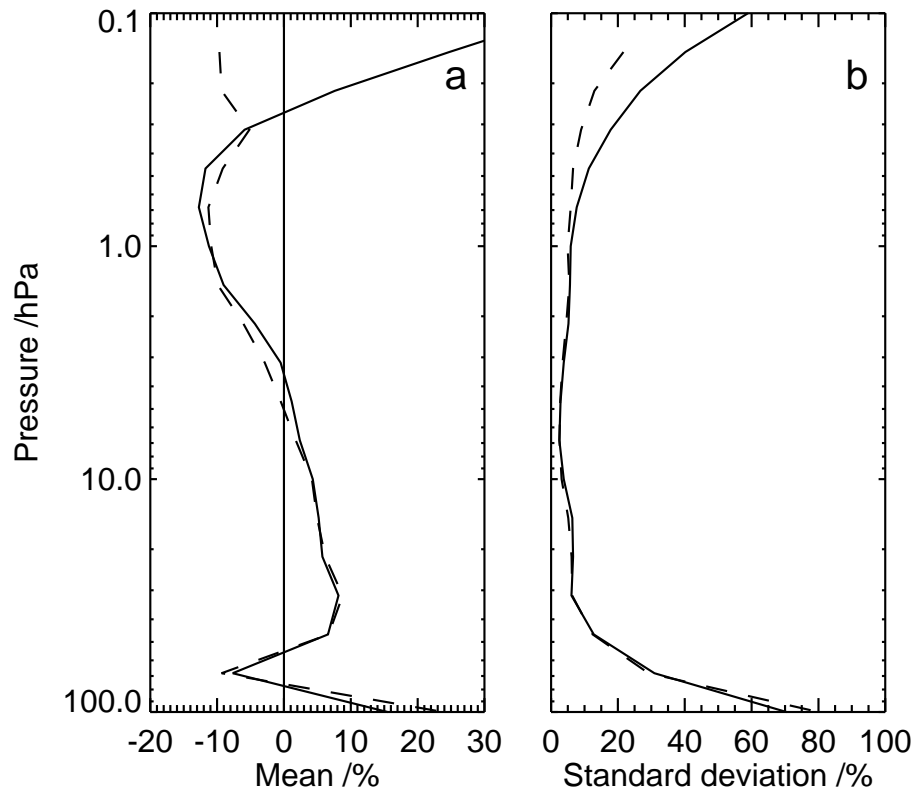


Fig. 9. BASCOE – HALOE ozone **(a)** bias and **(b)** standard deviation, calculated with a 12 h time window on the intercomparison grid (solid) and from the original model grid and with a time mismatch of less than 15 min (dashed). The averaging period is 18 August 2003 to 30 November 2003 and the region is 30° S to 30° N.

Intercomparison of ozone analyses

A. J. Geer et al.

Title Page

Abstract

Introduction

Conclusions

References

Tables

Figures

◀

▶

◀

▶

Back

Close

Full Screen / Esc

Printer-friendly Version

Interactive Discussion

Intercomparison of
ozone analyses

A. J. Geer et al.

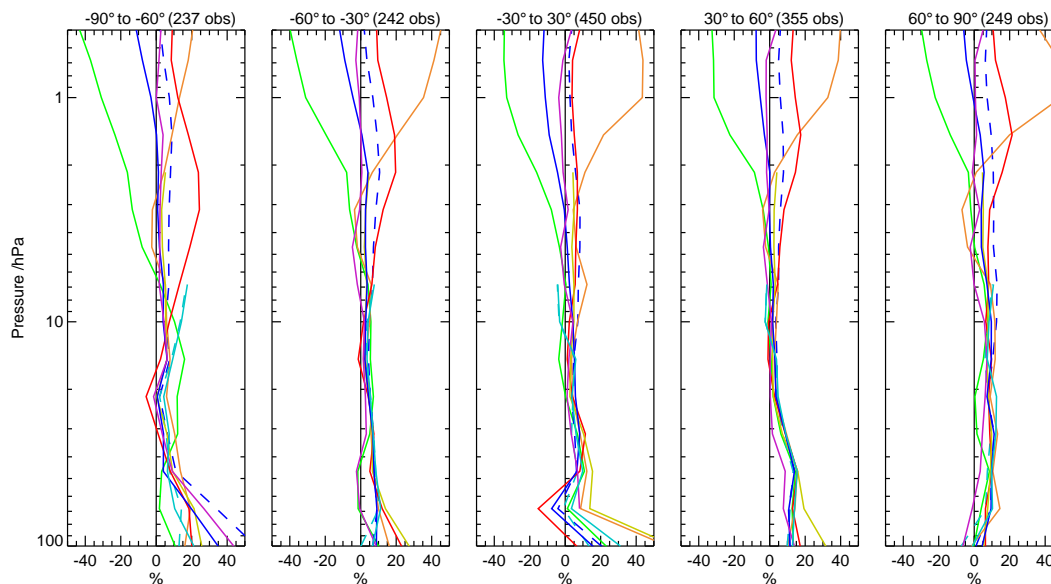


Fig. 10. Mean of (analysis – HALOE) ozone, normalised by climatology, in latitude bands for the period 18 August 2003 to 30 November 2003. Statistics are shown for the ECMWF MIPAS, DARC, KNMI TEMIS, BASCOE v3d24 and v3q33, MOCAGE-PALM Cariolle v2.1 and Reprobus, Juckes and MIMOSA analyses. See colour key in Fig. 3.

Title Page

Abstract

Introduction

Conclusions

References

Tables

Figures

◀

▶

◀

▶

Back

Close

Full Screen / Esc

Printer-friendly Version

Interactive Discussion

Intercomparison of
ozone analyses

A. J. Geer et al.

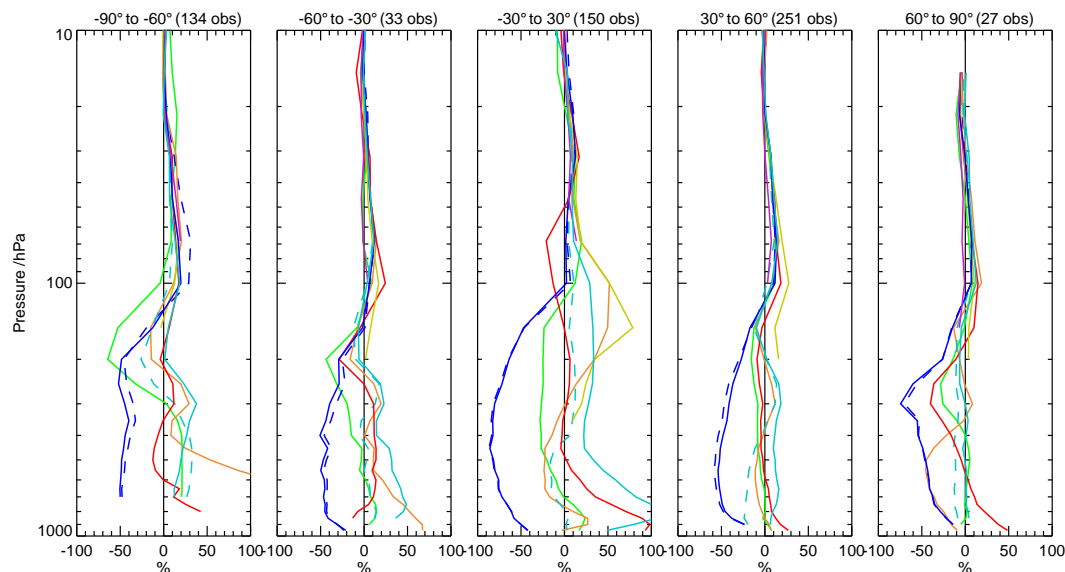


Fig. 11. Mean of (analysis – sonde) ozone, normalised by climatology, in latitude bands for the period 18 August 2003 to 30 November 2003. The analyses shown are the same as in Fig. 10; see colour key in Fig. 3.

[Title Page](#)[Abstract](#)[Introduction](#)[Conclusions](#)[References](#)[Tables](#)[Figures](#)[◀](#)[▶](#)[◀](#)[▶](#)[Back](#)[Close](#)[Full Screen / Esc](#)[Printer-friendly Version](#)[Interactive Discussion](#)

EGU

Intercomparison of
ozone analyses

A. J. Geer et al.

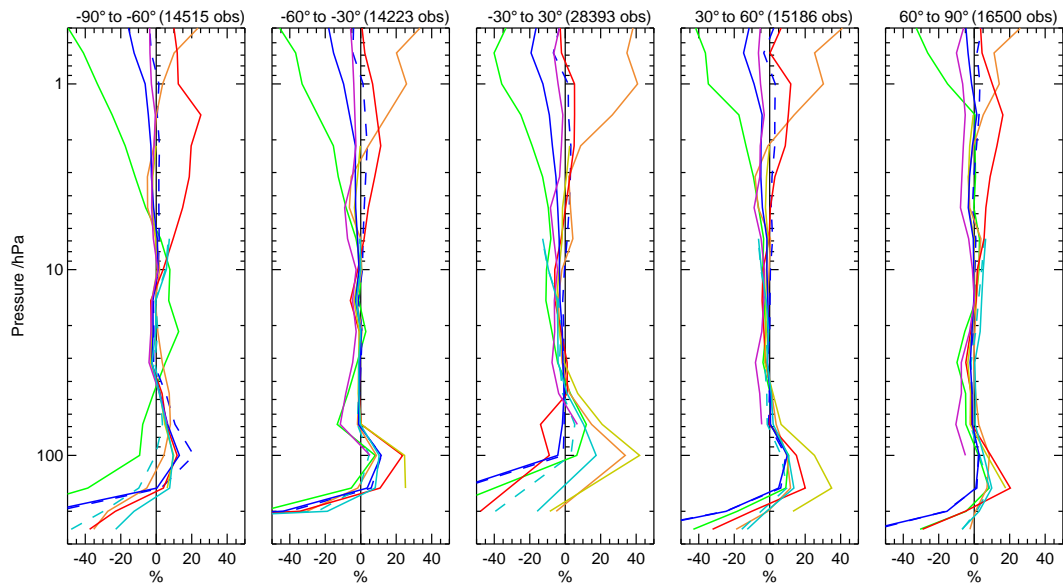


Fig. 12. Mean of (analysis – MIPAS) ozone, normalised by climatology, in latitude bands for the period 18 August 2003 to 30 November 2003. The analyses shown are the same as in Fig. 10; see colour key in Fig. 3.

[Title Page](#)[Abstract](#)[Introduction](#)[Conclusions](#)[References](#)[Tables](#)[Figures](#)[◀](#)[▶](#)[◀](#)[▶](#)[Back](#)[Close](#)[Full Screen / Esc](#)[Printer-friendly Version](#)[Interactive Discussion](#)

EGU

Intercomparison of
ozone analyses

A. J. Geer et al.

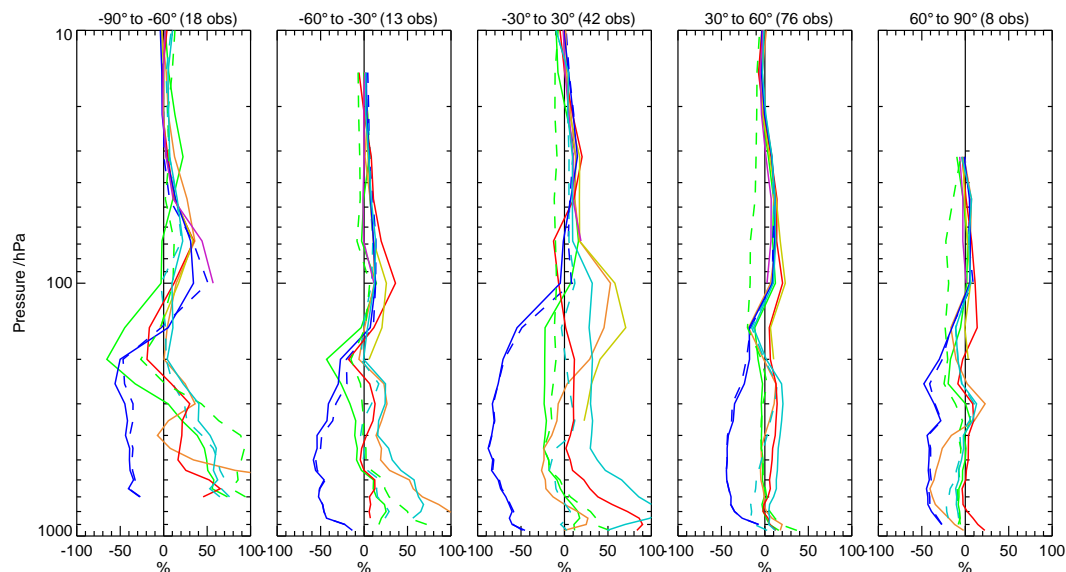


Fig. 13. Mean of (analysis – sonde) ozone, normalised by climatology, in latitude bands for the month of November 2003. The analyses shown are the same as in Fig. 10, but with the addition of the KNMI SCIAMACHY profile analyses; see colour key in Fig. 3.

[Title Page](#)[Abstract](#)[Introduction](#)[Conclusions](#)[References](#)[Tables](#)[Figures](#)[◀](#)[▶](#)[◀](#)[▶](#)[Back](#)[Close](#)[Full Screen / Esc](#)[Printer-friendly Version](#)[Interactive Discussion](#)

EGU

Intercomparison of
ozone analyses

A. J. Geer et al.

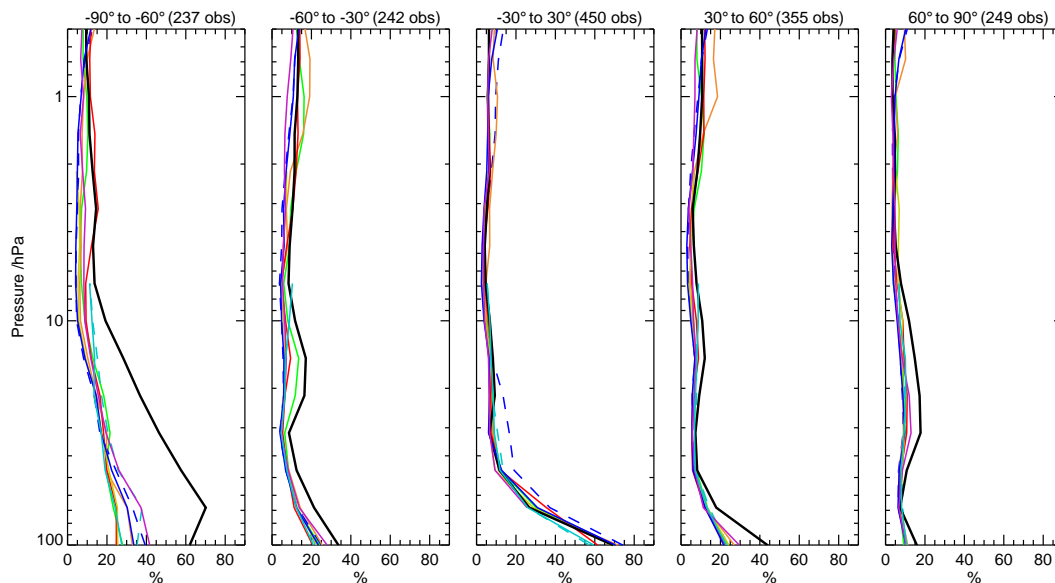


Fig. 14. Standard deviation of (analysis – HALOE) ozone, normalised by climatology, in latitude bands for the period 18 August 2003 to 30 November 2003. The analyses shown are the same as in Fig. 10, but with the addition of the Logan/Fortuin/Kelder climatology (black line); see colour key in Fig. 3.

[Title Page](#)[Abstract](#)[Introduction](#)[Conclusions](#)[References](#)[Tables](#)[Figures](#)[◀](#)[▶](#)[◀](#)[▶](#)[Back](#)[Close](#)[Full Screen / Esc](#)[Printer-friendly Version](#)[Interactive Discussion](#)

Intercomparison of
ozone analyses

A. J. Geer et al.

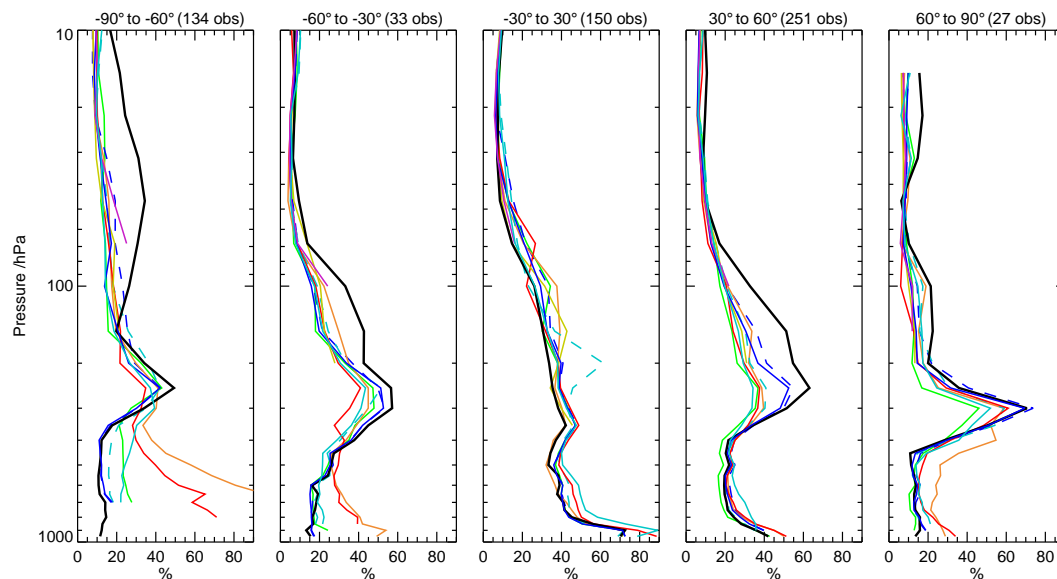


Fig. 15. Standard deviation of (analysis – sonde) ozone, normalised by climatology, in latitude bands for the period 18 August 2003 to 30 November 2003. The analyses shown are the same as in Fig. 10, but with the addition of the Logan/Fortuin/Kelder climatology (black line); see colour key in Fig. 3.

[Title Page](#)[Abstract](#)[Introduction](#)[Conclusions](#)[References](#)[Tables](#)[Figures](#)[◀](#)[▶](#)[◀](#)[▶](#)[Back](#)[Close](#)[Full Screen / Esc](#)[Printer-friendly Version](#)[Interactive Discussion](#)

EGU

Intercomparison of
ozone analyses

A. J. Geer et al.

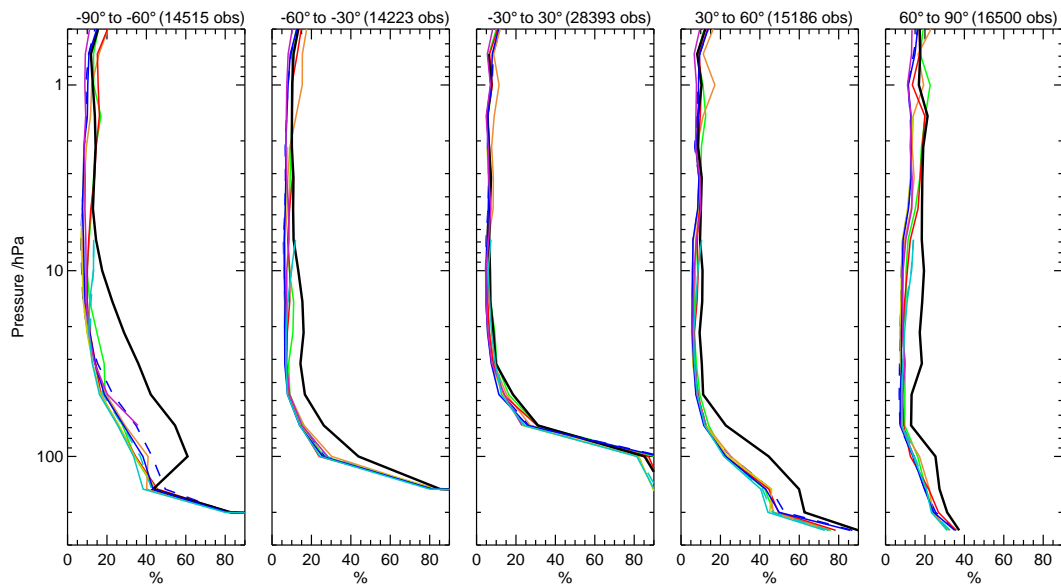


Fig. 16. Standard deviation of (analysis – MIPAS) ozone, normalised by climatology, in latitude bands for the period 18 August 2003 to 30 November 2003. The analyses shown are the same as in Fig. 10, but with the addition of the Logan/Fortuin/Kelder climatology (black line); see colour key in Fig. 3.

[Title Page](#)[Abstract](#)[Introduction](#)[Conclusions](#)[References](#)[Tables](#)[Figures](#)[◀](#)[▶](#)[◀](#)[▶](#)[Back](#)[Close](#)[Full Screen / Esc](#)[Printer-friendly Version](#)[Interactive Discussion](#)

EGU

Intercomparison of
ozone analyses

A. J. Geer et al.

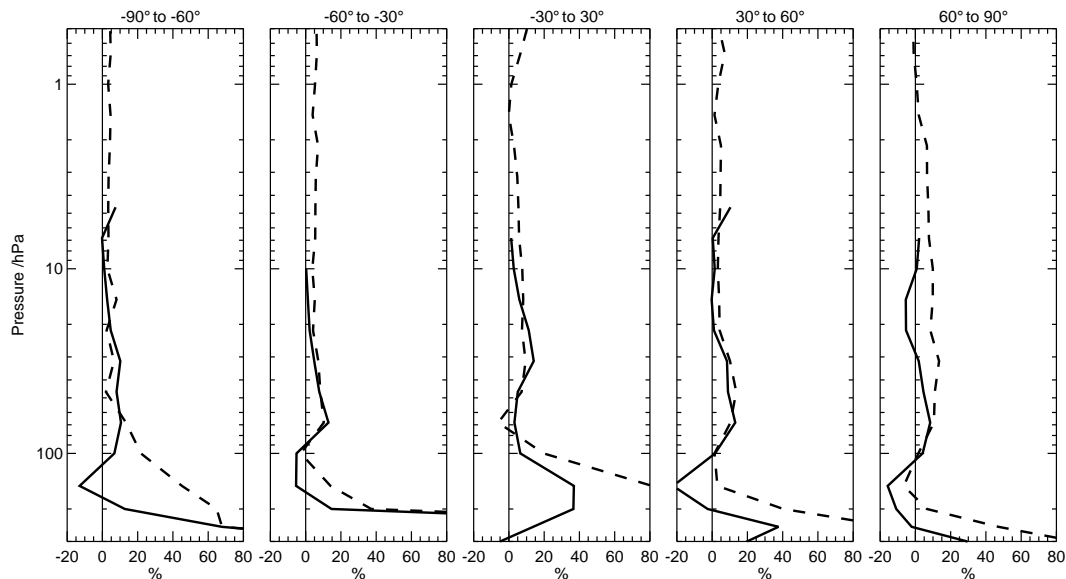


Fig. 17. Estimates of the mean of (MIPAS – sonde) (solid) and (MIPAS – HALOE) (dotted), using BASCOE v3q33 analyses as a transfer standard, and normalising by climatology, in latitude bands for the period 18 August 2003 to 30 November 2003.

[Title Page](#)[Abstract](#)[Introduction](#)[Conclusions](#)[References](#)[Tables](#)[Figures](#)[◀](#)[▶](#)[◀](#)[▶](#)[Back](#)[Close](#)[Full Screen / Esc](#)[Printer-friendly Version](#)[Interactive Discussion](#)

EGU

Intercomparison of
ozone analyses

A. J. Geer et al.

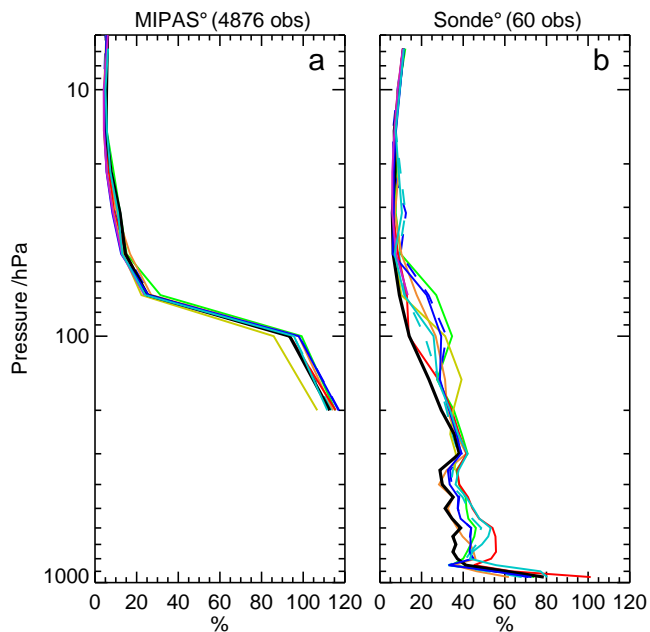


Fig. 18. Standard deviation of (a) (analysis – MIPAS) and (b) (analysis – sonde) ozone, normalised by climatology, in the latitude band 10° S to 0° for the period 18 August 2003 to 30 November 2003. The analyses shown are the same as in Fig. 10; see colour key in Fig. 3.

[Title Page](#)[Abstract](#)[Introduction](#)[Conclusions](#)[References](#)[Tables](#)[Figures](#)[◀](#)[▶](#)[◀](#)[▶](#)[Back](#)[Close](#)[Full Screen / Esc](#)[Printer-friendly Version](#)[Interactive Discussion](#)

EGU

Intercomparison of
ozone analyses

A. J. Geer et al.

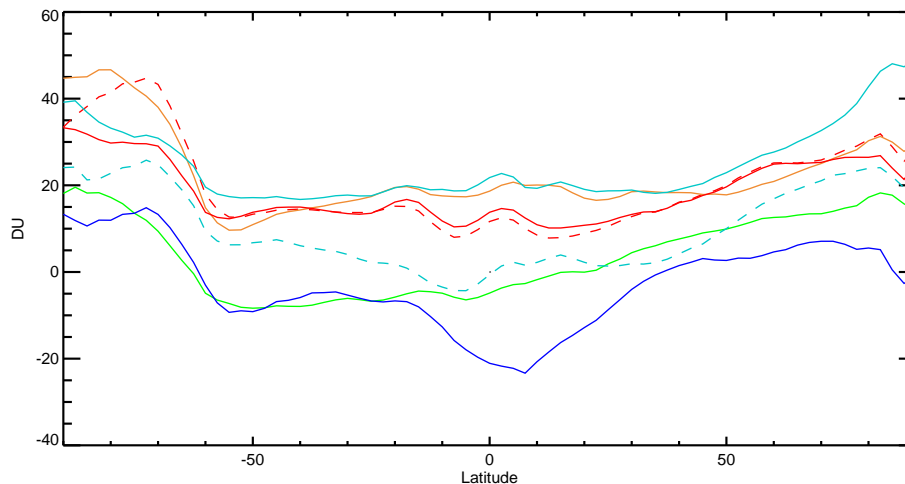


Fig. 19. Mean of (analysis – TOMS) total column ozone, in 5° latitude bins for the period 18 August 2003 to 30 November 2003. Shown are the ECMWF operational and MIPAS, MOCAGE-PALM Cariolle v2.1 and Reprobus, KNMI TEMIS, DARC and BASCOE v3q33 analyses. See colour key in Fig. 3.

[Title Page](#)[Abstract](#)[Introduction](#)[Conclusions](#)[References](#)[Tables](#)[Figures](#)[◀](#)[▶](#)[◀](#)[▶](#)[Back](#)[Close](#)[Full Screen / Esc](#)[Printer-friendly Version](#)[Interactive Discussion](#)

EGU

Intercomparison of
ozone analyses

A. J. Geer et al.

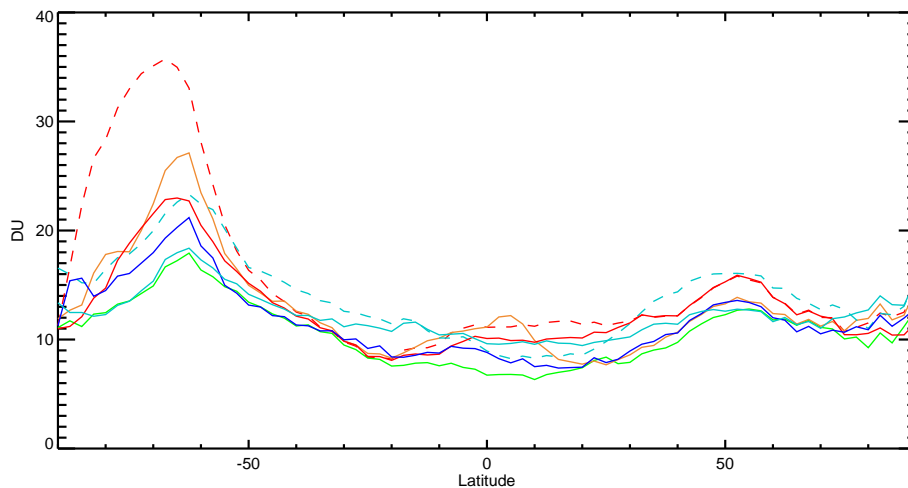


Fig. 20. Standard deviation of (analysis – TOMS) total column ozone, in 5° latitude bins for the period 18 August 2003 to 30 November 2003. Analyses shown are as Fig. 19; see colour key in Fig. 3.

[Title Page](#)[Abstract](#)[Introduction](#)[Conclusions](#)[References](#)[Tables](#)[Figures](#)[◀](#)[▶](#)[◀](#)[▶](#)[Back](#)[Close](#)[Full Screen / Esc](#)[Printer-friendly Version](#)[Interactive Discussion](#)

EGU

Intercomparison of
ozone analyses

A. J. Geer et al.

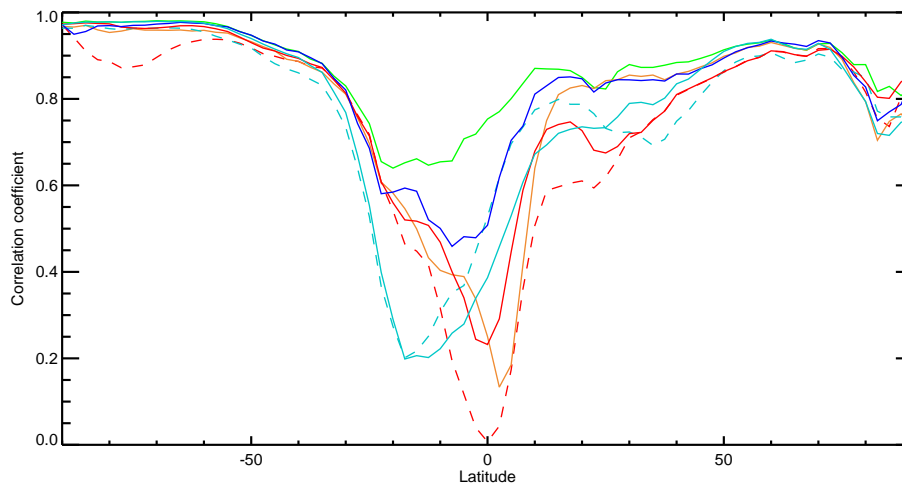


Fig. 21. Correlation coefficient of analysed against TOMS total column ozone, in 5° latitude bins for the period 18 August 2003 to 30 November 2003. Analyses shown are as Fig. 19; see colour key in Fig. 3.

[Title Page](#)[Abstract](#)[Introduction](#)[Conclusions](#)[References](#)[Tables](#)[Figures](#)[◀](#)[▶](#)[◀](#)[▶](#)[Back](#)[Close](#)[Full Screen / Esc](#)[Printer-friendly Version](#)[Interactive Discussion](#)

EGU

Intercomparison of
ozone analyses

A. J. Geer et al.

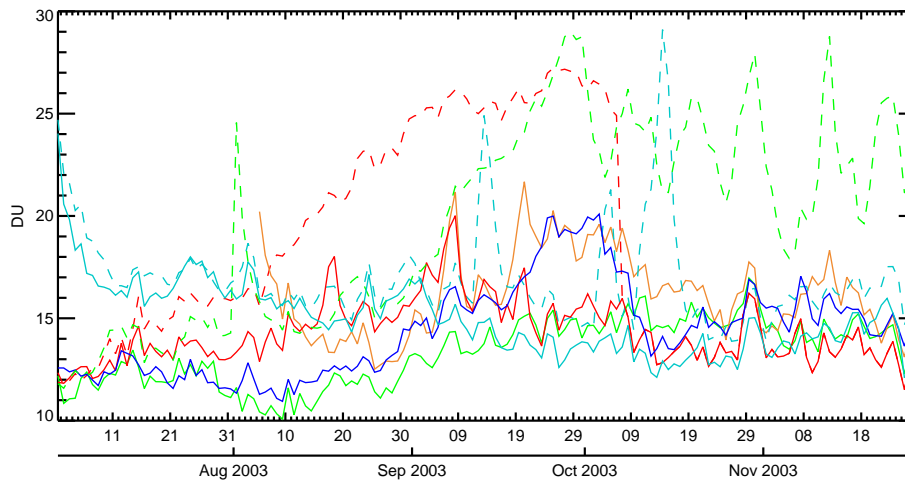


Fig. 22. Standard deviation of (analysis – TOMS) total column ozone, globally averaged, shown daily from 18 August 2003 to 30 November 2003. Analyses shown are as Fig. 19 but with the addition of the KNMI SCIAMACHY profile analyses; see colour key in Fig. 3.

[Title Page](#)[Abstract](#)[Introduction](#)[Conclusions](#)[References](#)[Tables](#)[Figures](#)[◀](#)[▶](#)[◀](#)[▶](#)[Back](#)[Close](#)[Full Screen / Esc](#)[Printer-friendly Version](#)[Interactive Discussion](#)

EGU

Intercomparison of
ozone analyses

A. J. Geer et al.

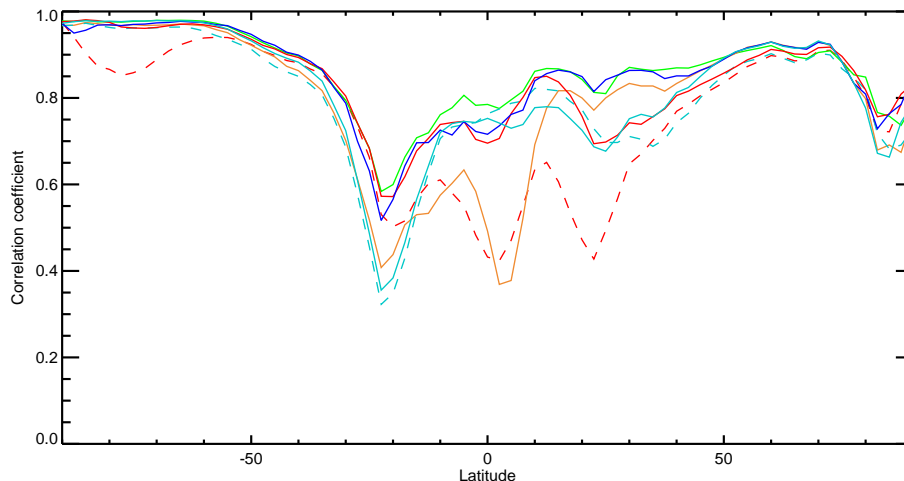


Fig. 23. Correlation coefficient of analysed against TOMS total column ozone, in 5° latitude bins for the period 18 August 2003 to 30 November 2003. Logan (1999) climatology ozone fields have been substituted into the analyses at 200 hPa and below. Analyses shown are as Fig. 19; see colour key in Fig. 3.

[Title Page](#)[Abstract](#)[Introduction](#)[Conclusions](#)[References](#)[Tables](#)[Figures](#)[◀](#)[▶](#)[◀](#)[▶](#)[Back](#)[Close](#)[Full Screen / Esc](#)[Printer-friendly Version](#)[Interactive Discussion](#)

EGU

Intercomparison of
ozone analyses

A. J. Geer et al.

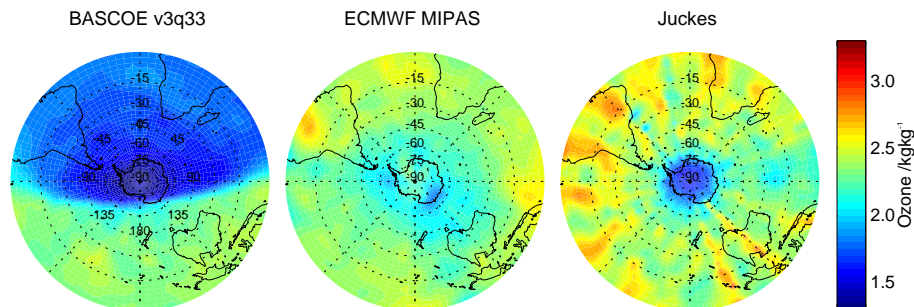


Fig. 24. Ozone analyses in the mesosphere at 0.32 hPa on 15 November 2003. Projection is polar stereographic, bounded by the equator and centred on the South Pole.

[Title Page](#)[Abstract](#)[Introduction](#)[Conclusions](#)[References](#)[Tables](#)[Figures](#)[◀](#)[▶](#)[◀](#)[▶](#)[Back](#)[Close](#)[Full Screen / Esc](#)[Printer-friendly Version](#)[Interactive Discussion](#)

EGU

Intercomparison of
ozone analyses

A. J. Geer et al.

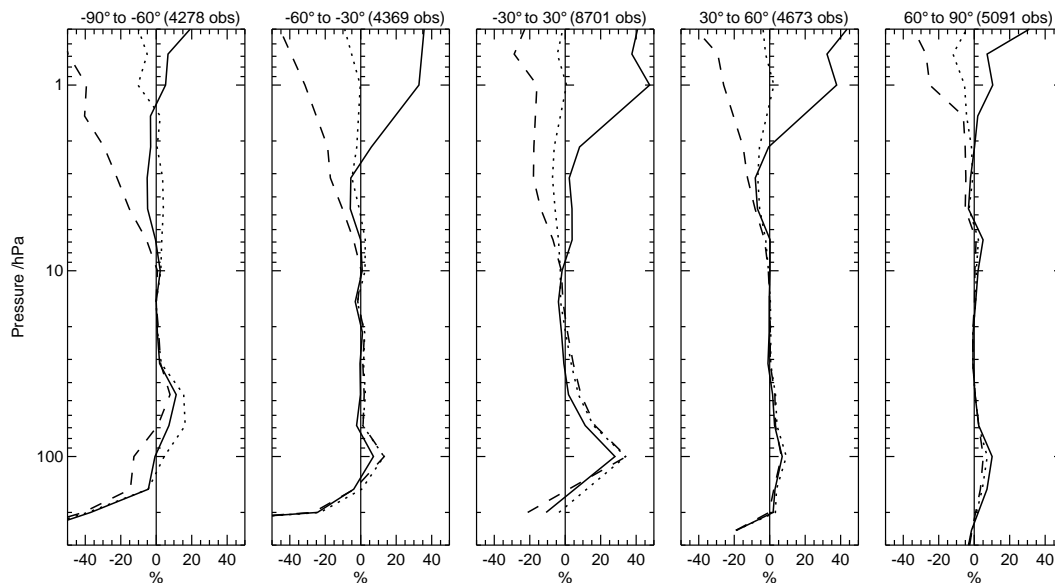


Fig. 25. Mean of (analysis – MIPAS) ozone, normalised by climatology, in latitude bands for the month of October 2003. Figure shows the DARC analyses (solid line), DARC analyses with a correctly implemented Cariolle v1.0 photochemistry scheme (dotted line) and DARC analyses with the LINOZ photochemistry scheme (dashed line).

[Title Page](#)[Abstract](#)[Introduction](#)[Conclusions](#)[References](#)[Tables](#)[Figures](#)[◀](#)[▶](#)[◀](#)[▶](#)[Back](#)[Close](#)[Full Screen / Esc](#)[Printer-friendly Version](#)[Interactive Discussion](#)

Intercomparison of
ozone analyses

A. J. Geer et al.

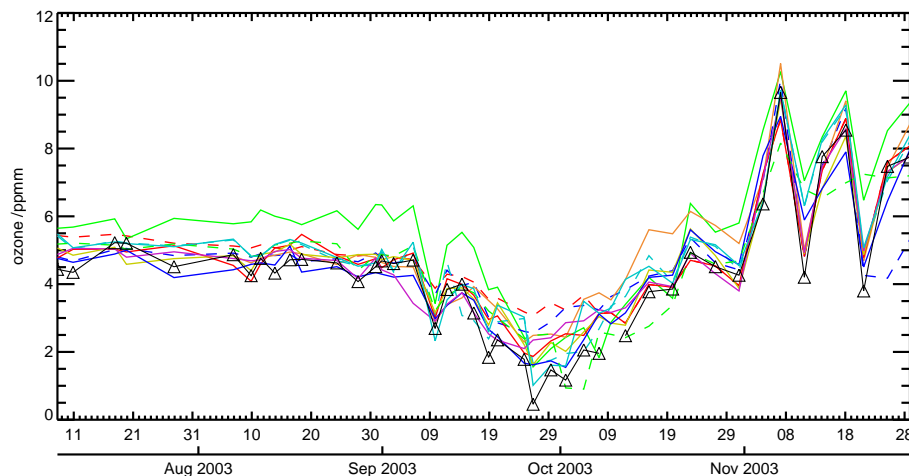


Fig. 26. Ozonesonde measurements (triangles joined by black line) and analyses (see key Fig. 3) at 32 hPa over the South Pole. Analysis points are only shown on days when the sonde made a measurement. Shown are the ECMWF operational and MIPAS, DARC, KNMI TEMIS and SCIAMACHY profile, BASCOE v3d24 and v3q33, MOCAGE-PALM Cariolle v2.1 and Reprobus, Juckes and MIMOSA analyses.

[Title Page](#)[Abstract](#)[Introduction](#)[Conclusions](#)[References](#)[Tables](#)[Figures](#)[◀](#)[▶](#)[◀](#)[▶](#)[Back](#)[Close](#)[Full Screen / Esc](#)[Printer-friendly Version](#)[Interactive Discussion](#)

EGU

Intercomparison of
ozone analyses

A. J. Geer et al.

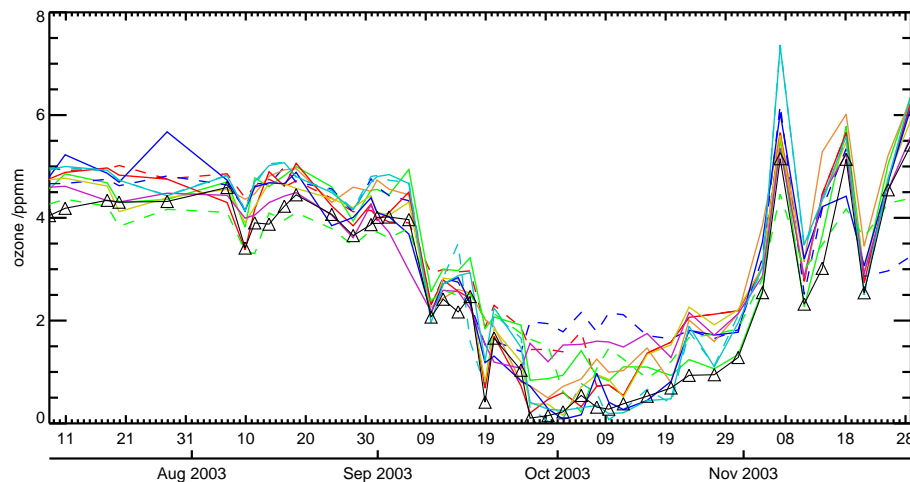


Fig. 27. Ozonesonde measurements (triangles joined by black line) and analyses (see key Fig. 3) at 46 hPa over the South Pole. Analysis points are only shown on days when the sonde made a measurement. Analyses shown are the same as in Fig. 26.

[Title Page](#)[Abstract](#)[Introduction](#)[Conclusions](#)[References](#)[Tables](#)[Figures](#)[◀](#)[▶](#)[◀](#)[▶](#)[Back](#)[Close](#)[Full Screen / Esc](#)[Printer-friendly Version](#)[Interactive Discussion](#)

EGU

Intercomparison of
ozone analyses

A. J. Geer et al.

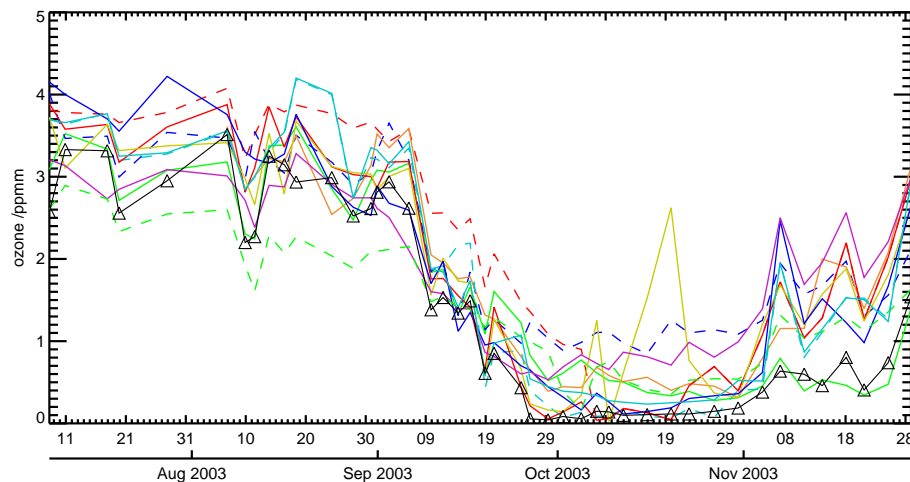


Fig. 28. Ozonesonde measurements (triangles joined by black line) and analyses (see key Fig. 3) at 68 hPa over the South Pole. Analysis points are only shown on days when the sonde made a measurement. Analyses shown are the same as in Fig. 26.

[Title Page](#)[Abstract](#)[Introduction](#)[Conclusions](#)[References](#)[Tables](#)[Figures](#)[◀](#)[▶](#)[◀](#)[▶](#)[Back](#)[Close](#)[Full Screen / Esc](#)[Printer-friendly Version](#)[Interactive Discussion](#)

EGU

Intercomparison of
ozone analyses

A. J. Geer et al.

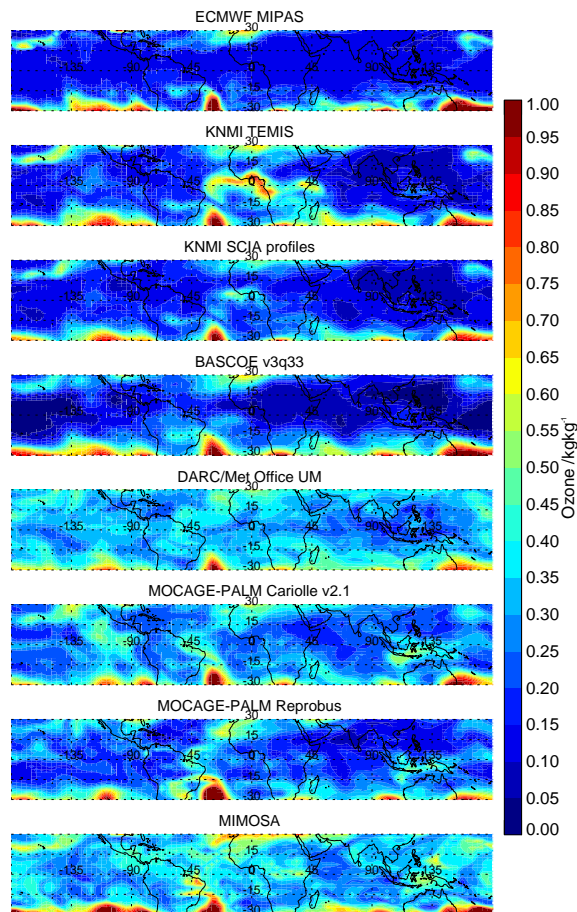


Fig. 29. Ozone analyses at 100 hPa on 17 October 2003, in ppmm, shown on a Mercator projection with a latitude range 30° S to 30° N about the equator.

[Title Page](#)[Abstract](#)[Introduction](#)[Conclusions](#)[References](#)[Tables](#)[Figures](#)[◀](#)[▶](#)[◀](#)[▶](#)[Back](#)[Close](#)[Full Screen / Esc](#)[Printer-friendly Version](#)[Interactive Discussion](#)